

IMMUNOBIOLOGY AND IMMUNOTHERAPY

IL-7 receptor signaling drives human B-cell progenitor differentiation and expansion

Fabian M. P. Kaiser,^{1,*} Iga Janowska,^{2,3,*} Roberta Menafra,^{4,†} Melanie de Gier,^{5,†} Jakov Korzhenevich,⁶ Ingrid Pico-Knijnenburg,⁵ Indu Khatri,⁷ Ansgar Schulz,⁸ Taco W. Kuijpers,⁹ Arjan C. Lankester,¹⁰ Lukas Konstantinidis,¹¹ Miriam Erlacher,¹² Susan Kloet,⁴ Pauline A. van Schouwenburg,⁵ Marta Rizzi,^{2,3,6,13,‡} and Mirjam van der Burg^{5,‡}

¹Department of Immunology, Erasmus University Medical Center, Rotterdam, The Netherlands; ²Department of Rheumatology and Clinical Immunology, Freiburg University Medical Center, University of Freiburg, Freiburg, Germany; ³Center for Chronic Immunodeficiency, University Medical Center Freiburg, Faculty of Medicine, University of Freiburg, Freiburg, Germany; ⁴Leiden Genome Technology Center, Leiden, The Netherlands; ⁵Department of Pediatrics, Laboratory for Pediatric Immunology, Willem-Alexander Children's Hospital, Leiden University Medical Center, Leiden, The Netherlands; ⁶Division of Clinical and Experimental Immunology, Institute of Immunology, Center for Pathophysiology, Infectiology and Immunology, Medical University of Vienna, Vienna, Austria; ⁷Department of Immunology, Leiden University Medical Center, Leiden, The Netherlands; ⁸Department of Pediatrics and Adolescent Medicine, University Medical Center, University Ulm, Ulm, Germany; ⁹Department of Pediatrics, Amsterdam University Medical Center, Amsterdam, The Netherlands; ¹⁰Department of Pediatrics, Hematology and Stem Cell Transplantation, Willem-Alexander Children's Hospital, Leiden University Medical Center, Leiden, The Netherlands; ¹¹Department of Orthopedics and Trauma Surgery, ¹²Division of Pediatric Hematology and Oncology, Department of Pediatrics and Adolescent Medicine, Freiburg University Medical Center, University of Freiburg, Freiburg, Germany; and ¹³Centre for Integrative Biological Signalling Studies, University of Freiburg, Freiburg, Germany

KEY POINTS

- IL-7 induces a strong proliferative burst in early human B-cell progenitors but has a limited role in the prevention of cell death.
- IL-7 enhances *BACH2*, *EBF1*, and *PAX5* expression in early B-cell progenitors, which specify and commit early progenitors to the B-cell fate.

Although absence of interleukin-7 (IL-7) signaling completely abrogates T and B lymphopoiesis in mice, patients with severe combined immunodeficiency caused by mutations in the IL-7 receptor α chain (IL-7R α) still generate peripheral blood B cells. Consequently, human B lymphopoiesis has been thought to be independent of IL-7 signaling. Using flow cytometric analysis and single-cell RNA sequencing of bone marrow samples from healthy controls and patients who are IL-7R α deficient, in combination with in vitro modeling of human B-cell differentiation, we demonstrate that IL-7R signaling plays a crucial role in human B lymphopoiesis. IL-7 drives proliferation and expansion of early B-cell progenitors but not of pre-BII large cells and has a limited role in the prevention of cell death. Furthermore, IL-7 guides cell fate decisions by enhancing the expression of *BACH2*, *EBF1*, and *PAX5*, which jointly orchestrate the specification and commitment of early B-cell progenitors. In line with this observation, early B-cell progenitors of patients with IL-7R α deficiency still expressed myeloid-specific genes. Collectively, our results unveil a previously unknown role for IL-7 signaling in promoting the B-lymphoid fate and expanding early human B-cell progenitors while defining important differences between mice and humans. Our results have implications for hematopoietic stem cell transplantation strategies in patients with T⁻ B⁺ severe combined immunodeficiency and provide insights into the role of IL-7R signaling in leukemogenesis.

Implications for hematopoietic stem cell transplantation strategies in patients with T⁻ B⁺ severe combined immunodeficiency and provide insights into the role of IL-7R signaling in leukemogenesis.

Introduction

The early stages of murine B lymphopoiesis occur in close proximity to bone marrow (BM) stromal cells that produce high levels of interleukin-7 (IL-7),¹ which is essential for development beyond the pre-pro-B-cell stage.²⁻⁶ IL-7 signaling is transmitted through the IL-7 receptor (IL-7R), which consists of the IL-7-specific IL-7R α chain (CD127) and the common gamma (γ) chain (CD132), and initiates nonredundant but complementary signaling pathways that promote B-lineage specification, proliferation, and survival of early B-cell progenitors (BCPs) by mainly activating JAK/STAT5 and PI3K/AKT signaling pathways.⁷ In this model, a transient pulse of IL-7 signaling has been

suggested to induce *Ebf1* and *Pax5* expression at the transition from the all-lymphoid progenitor (ALP) to B-cell-biased lymphoid progenitor (BLP) stage to promote B-lymphocyte specification,⁸ after which expression of both B-cell-specific transcription factors is thought to be sustained via a positive feedback loop that does not require continued exposure to IL-7.⁷ In addition, IL-7 signaling upregulates expression of the cell cycle regulator cyclin D3, which drives proliferation of early BCPs^{9,10} and induces the metabolic programs that are required for expansion of the progenitor pool.¹¹ Upon successful recombination of the immunoglobulin (Ig) heavy-chain locus, the proliferative signals of the IL-7R synergize with pre-B-cell receptor (pre-BCR) signaling to induce a strong proliferative

burst until IL-7R signaling is attenuated by the pre-BCR as the cells proceed to Ig light chain rearrangement.^{7,12} In addition, IL-7R signaling upregulates pro-survival factors and concomitantly downregulates proapoptotic proteins¹³⁻¹⁶ and has been implicated in *Igh* repertoire diversification both at the diversity (D_H) to joining (J_H) and variable (V_H) to DJ_H stages of recombination¹⁷ while simultaneously suppressing premature recombination of the *Igk* locus.^{16,18}

Whereas IL-7 signaling is absolutely required for B lymphopoiesis in mice, human IL-7R α chain deficiency manifests as T⁻ B⁺ natural killer cell (NK)-positive severe combined immunodeficiency (SCID) and patients with deleterious mutations in the IL-7R α chain generate peripheral blood B cells.^{19,20} Thus, human B lymphopoiesis seems to be less dependent on IL-7 signaling and several studies aimed at unraveling its function, which were mostly based on the *in vitro* differentiation of human hematopoietic progenitors in xenogeneic or syngeneic culture systems, have yielded partially conflicting results.²¹⁻²⁶ IL-7 signaling was also postulated to induce terminal deoxynucleotidyltransferase (TdT) expression and *IGH* junctions of IL-7R α deficient patients were found to have less N-nucleotides.²⁷ Importantly, constitutively active IL-7R signaling leads to B-cell acute lymphoblastic leukemia,²⁸⁻³² supporting the hypothesis that IL-7 signaling may play an important role in human B lymphopoiesis. However, a clear picture about the role of IL-7 in human B lymphopoiesis is currently lacking. As a consequence, patients with T⁻ B⁺ SCID with defects in IL-7 signaling often do not receive chemotherapeutic conditioning before hematopoietic stem cell transplantation (HSCT), assuming that autologous early BCPs do not have to be eradicated in order to acquire full humoral immunocompetence after transplantation.^{33,34}

Here, we demonstrate a critical role for IL-7 signaling in human B lymphopoiesis by promoting human BCP differentiation and expansion.

Methods

BM samples for ex vivo flow cytometry and scRNA-seq

BM samples for flow cytometry were isolated from pediatric controls who have previously been described.³⁵ The 2 pediatric controls used for single-cell RNA sequencing (scRNA-seq) were healthy donors at the age of 2.5 years for BM transplantation of diseased siblings. Approval for obtaining the samples was provided by the local ethics committee of the Leiden University Medical Center (protocol P018.028). BM samples of the 2 patients with IL-7R α -deficient SCID were obtained at the ages of 3 and 9 months, respectively, with informed consent to analyze and publish the data as provided by the parent/guardian. One patient had a homozygous premature nonsense mutation in the *IL7RA* gene (c.208G>T; p.E70X), whereas the other patient had a heterozygous splice acceptor site mutation (c.83-2A>G) and a chromosomal deletion of the other allele.

Flow cytometric analysis of human BM samples

Analysis was performed using previously frozen BM. Cells were stained with 2 different antibody panels, using either the FIX & PERM cell permeabilization kit (Invitrogen) or the eBioscience Foxp3/transcription factor staining buffer set (Invitrogen)

according to the manufacturer's instructions. Briefly, cells were thawed in Hanks balanced salt solution, supplemented with 3% fetal bovine serum (Gibco) and 2.5 mM CaCl₂, and were washed prior to incubation with antibodies targeting surface antigens and Annexin V for 20 minutes at 4°C. After washing, cells were fixed with the respective fixation agent according to the manufacturer's protocol before staining for intracellular or intranuclear antigens. The staining for PAX5 and intranuclear antigens was performed with the eBioscience Foxp3/transcription factor staining buffer set (Invitrogen) for 1 hour at 4°C. After 2 final washing steps, samples were acquired on a BD LSR Fortessa cell analyzer (BD Biosciences). Data analysis was performed with FlowJo version 10.8.1 (TreeStar). The following marker combinations were used for the definition of the populations: common lymphoid progenitors (CLPs; CD34⁺, CD10⁺, CD38⁺, CD19⁻, and TdT⁻, with or without cytoplasmic CD79A⁻), pro-B (CD34⁺, CD10⁺, CD38⁺, CD19⁻, and TdT⁺, with or without cytoplasmic CD79A⁺), pre-BI (CD34⁺, CD10⁺, CD38⁺, and CD19⁺), pre-BII large (CD34⁻, CD10⁺, CD38⁺, CD19⁺, surface IgM⁻, and cytoplasmic CD179A⁺ and Ki-67⁺ or FSC-A^{high}), pre-BII small (CD34⁻, CD10⁺, CD38⁺, CD19⁺, surface IgM⁻, and cytoplasmic CD179A⁻ and Ki-67⁻ or FSC-A^{small}), immature (CD34⁻, CD10⁺, CD38⁺, CD19⁺, surface IgM⁺, and IgD⁻), and transitional (CD34⁻, CD10⁺, CD38⁺, CD19⁺, surface IgM⁺, and IgD⁺).

In vitro differentiation of B lymphocytes

Umbilical cord blood (CB) and BM samples were obtained upon signed informed consent and approval by the University Freiburg ethics committee (353/07_120590 or 20-1109, respectively). Donors for BM samples for the *in vitro* differentiation of BCP were otherwise healthy males aged 47, 49, and 67 years, undergoing hip replacement surgery. CD34⁺ cells were isolated from CB by positive selection with the CD34⁺ MicroBead kit (Miltenyi Biotec), following the manufacturer's protocol. Isolated CD34⁺ cells were plated at 0.1 × 10⁶ cells per mL in 96-well U-bottom plates in Iscove medium containing fetal bovine serum (10%), L-glutamine (1×), nonessential amino acids (1%), reduced glutathione (1 µg/mL), transferrin (2.5 µg/mL), and insulin (1 µg/mL), as previously described.³⁶ After isolation, the medium was supplemented with IL-6, stem cell factor (SCF), and FMS-like tyrosine kinase 3 ligand (Flt3L) (all at 25 ng/mL; Immunotools). On day 7 of culture, SCF and Flt3L (25 ng/mL) were added again; medium for control cultures additionally contained IL-7 (20 ng/mL; Immunotools). From day 14 onward, the cells were kept in a cytokine-free medium, and half of the medium was refreshed twice a week.

The following marker combinations were used for the definition of the populations: CLP (CD33⁻, CD10⁺, CD38⁺, cytoplasmic CD79A⁻, and CD19⁻), pro-B (CD33⁻, CD10⁺, CD38⁺, cytoplasmic CD79A⁺, and CD19⁻), pre-BI (CD33⁻, CD10⁺, CD38⁺, cytoplasmic CD79A⁺, CD19⁺, cytoplasmic IgM⁻, and surface IgM⁻), pre-BII large (CD33⁻, CD10⁺, CD38⁺, cytoplasmic CD79A⁺, CD19⁺, cytoplasmic IgM⁺, surface IgM⁻, Ki-67⁺, and cytoplasmic CD179A⁺), pre-BII small (CD33⁻, CD10⁺, CD38⁺, cytoplasmic CD79A⁺, CD19⁺, cytoplasmic IgM⁺, surface IgM⁻, Ki-67⁻, and cytoplasmic CD179A⁻), and immature B cells (CD33⁻, CD10⁺, CD38⁺, cytoplasmic CD79A⁺, CD19⁺, cytoplasmic IgM⁺, and surface IgM⁺). Staining of specific antigens was performed with the eBioscience Foxp3/transcription factor staining buffer set according to the manufacturer's protocol

(Invitrogen). Three wells of each condition were pooled at each time point. Staining of intracellular antigens was performed for 30 minutes at room temperature. For anti-EBF1 staining, samples were additionally incubated with an anti-rabbit AF647-conjugated secondary antibody for 15 minutes at 4°C. Samples were acquired on a Cytex Aurora (Cytex Biosciences), using SpectroFlo software (version 2.2.0.3). Data analysis was performed with FlowJo version 10.7 (TreeStar). Gated populations containing <10 cells were excluded from analysis. Replicates were treated as individual measurements.

Sample preparation for scRNA-seq

Analysis was performed with previously frozen material that was enriched for BM mononuclear cells via Ficoll density centrifugation before freezing. BM mononuclear cells of the 2 aforementioned pediatric controls and the 2 patients with IL-7R α -deficient SCID were thawed and dead cells were removed with the Dead Cell Removal kit (Miltenyi Biotec) according to the manufacturer's instructions. Subsequently, non-B cells were depleted using the MojoSort Human Pan B-Cell Isolation kit (BioLegend). After the addition of Fc block (eBioscience), cells were labeled in phosphate-buffered saline with 1% bovine serum albumin using the following TotalSeq-C antibodies (BioLegend): 0050 anti-human CD19 (clone HIB19), 0054 anti-human CD34 (clone 581), 0136 anti-human IgM (clone MHM-88), and 0390 anti-human CD127 (clone A019D5).

Single-cell library preparation and sequencing

Single-cell gene expression libraries were generated via the 10x Genomics Chromium platform, using the Chromium Next GEM Single Cell 5' Library & Gel Bead kit version 1.1 and Chromium Next GEM Chip G Single Cell kit (10x Genomics) according to the manufacturer's protocol. Targeted BCR libraries were generated using the Chromium Single Cell V(D)J Enrichment kit for human B cells and the Chromium Single Cell 5' Library Construction kit (10x Genomics) according to the manufacturer's protocol. Cellular indexing of transcriptomes and epitopes by sequencing (CITE-seq) libraries were generated using the Chromium Single Cell 5' Feature Barcode Library Kit (10x Genomics) according to the manufacturer's protocol. Gene expression, targeted BCR, and CITE-seq libraries were sequenced on a NovaSeq 6000 S4 flow cell, using version 1 chemistry (Illumina).

Data analysis

For library demultiplexing, FASTQ file generation, and read alignment, CellRanger software version 3.1 was used with feature barcoding function. Resulting matrixes contained the number of unique molecular identifiers (UMIs) per genes or per antibody for each cell. The gene expression and antibody matrixes of the 4 samples were imported in Seurat version 3,³⁷ retaining only genes expressed in at least 3 cells, and merged into a combined Seurat object. Cells with <250 UMIs or <3000 genes and >25% of mitochondrial RNAs were filtered out. Random selection of an equal amount of cells per patient was chosen to minimize sample bias. Antibody UMI counts were centered using log ratio normalization to account for unspecific background.

In order to identify shared clusters of cells collected from different groups (patients and controls), the gene-barcode

matrix was integrated according to the integration workflow in Seurat,³⁷ using SCT-transform to normalize and scale the gene expression. Next, principal components analysis and uniform manifold approximation and projection (UMAP) were performed, and 30 principal components were used as input for graph-based clustering (resolution = 0.8). In order to assign the resulting 19 clusters to a cell type, we analyzed the results of the "FindAllMarkers" function and the expression of marker genes, such as lineage-specific transcription factors or markers used for the definition of populations in flow cytometry. Clusters 5, 9, and 12 were merged into a pre-BII large cluster based on their gene expression signature, similar expression of pre-BII cell large cell markers, and genes associated with proliferation. Clusters 0 and 1 were merged into a pre-BII small cluster based on their gene expression signature and similar expression of pre-BII small cell markers. The late-stage cluster contained cells with weak expression of B-cell markers and could represent cells with unsuccessful *IGH* or *IGK/IGL* rearrangements or preapoptotic cells. It was therefore excluded from further analyses.

Clusters CLP/pro-B1, pro-B2, pro-B3, and pro-B4/pre-BI displayed the typical signature of early lymphoid and B-cell progenitors and constituted the early BCP subset together with the lymphomyeloid-primed progenitor (LMPP) cluster. Clusters pro-B4/pre-BI, pre-BII large, pre-BII small, and immature were defined as the late BCP subset. The UMAP embedding was then used as input for pseudotime analysis using slingshot version 2.2.1³⁸: the LMPP cluster was used as a starting point for the early BCP subset, and cluster pro-B4/pre-BI was chosen as a starting point for the late BCP subset. After calculating the pseudotime, the cells were ordered along the resulting trajectories. To analyze how the progression along the pseudotime is affected by IL-7R α deficiency, we performed a univariate analysis of the pseudotime values between the 2 groups (patients and controls) using slingshot version 2.2.1³⁸ and the latest tradeSeq package (version 1.7.07),³⁹ following the transforming growth factor- β (TGF β) example.⁴⁰

Differences between the proportion of cells in the individual clusters between controls and patients were determined with a single-cell proportion test.⁴¹

In order to identify differentially expressed genes between conditions in each cell type, a combined metadata field was added to the 2 subsets, which contained the combination of the cluster name and the condition (patient/control). For this analysis, we used the "FindMarkers" function in Seurat. Data for all clusters are available in supplemental Tables 1-15, available on the *Blood* website.

For gene set enrichment analysis (GSEA), the fgsea package version 1.20 was used: firstly, we identified differentially expressed genes between patients and controls per cluster using the FindMarkers function (with these settings: logfc.threshold = 0.2; min.pct = 0.1; and min.diff.pct = 0) (supplemental Tables 1-15). Each gene list was then ranked based on the average difference in gene expression between patient and control. Ranked lists were used as input for GSEA, and the gene sets were obtained from the Molecular Signature database (MSigDB).

IGH repertoire sequencing of naive mature B cells

For the analysis of *IGH* rearrangements, naive mature B cells (defined as CD19⁺, CD27⁻, IgD⁺, CD24⁻, and CD38⁻) were sorted using the peripheral blood of patients with SCID and 3 age-matched healthy controls after Ficoll density centrifugation on a BD FACSAria III (BD Biosciences). All patients with JAK3-deficient or γ -deficient SCID and controls were aged between 4 and 7 months. DNA was isolated using direct lysis,⁴² and *IGH* rearrangements were amplified as previously described.^{43,44} In short, *IGH* rearrangements were amplified via multiplex polymerase chain reaction (PCR) using the forward V_H1-6 FR1 and reverse J_H consensus BIOMED-2 primers.⁴⁵ After PCR amplification of the *IGH* gene rearrangements, PCR products were purified with the MinElute gel extraction kit (Qiagen) and Agencourt AMPure XP beads (Beckman Coulter). Subsequently, the concentration of the PCR product was measured using the Quant-it Picogreen dsDNA assay (Invitrogen). The purified PCR products were sequenced on the 454 GS junior instrument (Roche) using the Lib-A V2 kit (Roche) according to the manufacturer's recommendations.⁴⁶ Sequences were demultiplexed based on their multiplex identifier sequence and trimmed using ARGalaxy or custom scripts.⁴⁷ FastA files were uploaded to IMG/High-V-Quest,⁴⁸ and IMG/High-V-Quest output files were analyzed in ARGalaxy.⁴⁷ Only sequences with a unique V gene, J gene, and CDR3 nucleotide sequence were included. The repertoire diversity score was calculated according to Boyd et al.⁴⁹

Statistical analysis

Statistical analysis of the data was performed with GraphPad Prism version 9.4.1.

Antibodies

AF647 AffiniPure F(ab')₂ fragment donkey anti-rabbit IgG (H + L), Jackson ImmunoResearch Labs, catalog number 711-606-152, RRID:AB_2340625; AF647 mouse monoclonal antihuman Ki-67 (clone Ki-67), BioLegend, catalog number 350510, RRID:AB_10900821; AF700 mouse monoclonal anti-human Ki-67 (clone Ki-67), BioLegend, catalog number 350530, RRID:AB_2564040; allophycocyanin (APC) mouse monoclonal anti-human CD27 (clone L128), BD Biosciences, catalog number 337169, RRID:AB_647368; APC mouse monoclonal anti-human CD34 (clone 8G12), BD Biosciences, catalog number 345804, RRID:AB_2686894; APC-Cy7 mouse monoclonal antihuman CD19 (clone HIB19), BioLegend, catalog number 302218, RRID:AB_314248; APC-H7 mouse monoclonal anti-human CD10 (clone HI10A), BD Biosciences, catalog number 655404, RRID:AB_2870372; APC-R700 mouse monoclonal anti-human CD127 (clone HIL-7R-M21), BD Biosciences, catalog number 565185, RRID:AB_2739099; BV421 mouse monoclonal anti-human CD127 (clone HIL-7R-M21), BD Biosciences, catalog number 562437, RRID:AB_11153481; BV421 mouse monoclonal anti-human CD179a (clone HSL96), BD Biosciences, catalog number 566583, RRID:AB_2739748; BV421 mouse monoclonal anti-human CD20 (clone 2H7), BioLegend, catalog number 302330, RRID:AB_10965543; BV510 mouse monoclonal anti-human IgM (clone MHM-88), BioLegend, catalog number 314522, RRID:AB_2562916; BV605 mouse monoclonal anti-human CD38 (clone HIT2), BioLegend, catalog number 303532, RRID:AB_2562915; BV605 mouse monoclonal anti-human IgM (clone MHM-88), BioLegend, catalog number

314524, RRID:AB_2562374; BV711 mouse monoclonal anti-human CD10 (clone HI10a), BioLegend, catalog number 312226, RRID:AB_2565876; BV711 mouse monoclonal anti-human CD24 (clone ML5), BD Biosciences, catalog number 563401, RRID:AB_2631261; BV785 mouse monoclonal anti-human IgM (clone MHM-88), BioLegend, catalog number 314544, RRID:AB_2800832; BV786 mouse monoclonal anti-human Ki-67 (clone B56), BD Biosciences, catalog number 563756, RRID:AB_2732007; Cy5.5 annexin V, BD Biosciences, catalog number 559935, RRID:AB_2869268; Fluorescein (FITC) mouse monoclonal anti-human CD79A (clone HM47), BioLegend, catalog number 333512, RRID:AB_2565984; FITC mouse monoclonal anti-human IgD (clone ia6-2), BioLegend, catalog number 348206, RRID:AB_10612567; FITC mouse monoclonal anti-human TdT (clone HT6), Supertechs, catalog number 6600; human BD Fc Block, BD Biosciences, catalog number 564220, RRID:AB_2869554; mouse IgG1, κ isotype control, BD Biosciences, catalog number 562438, RRID:AB_11207319; Pacific Blue (PB) mouse monoclonal anti-human CD38 (clone HIT2), EXBIO Praha, catalog number PB-366-T100, RRID:AB_10736773; PC7 mouse monoclonal anti-human CD19 (clone J3-119), Beckman Coulter, catalog number IM3628U, RRID:AB_10638575; Phycoerythrin (PE) mouse monoclonal anti-human CD179A (clone HSL96), Milteny Biotec, catalog number 130-120-136, RRID:AB_2784019; PE mouse monoclonal anti-human CD79A (clone HM57), Agilent Technologies, catalog number R715901-2; PE mouse monoclonal anti-human TdT (cloneE17-1519), BD Biosciences, catalog number 332790, RRID:AB_2868637; PE-CF594 mouse monoclonal anti-human IgD (clone IA6-2), BD Biosciences, catalog number 562540, RRID:AB_11153129; PE-CF594 rat monoclonal anti-human PAX5 (clone 1H9), BD Biosciences, catalog number 562815, RRID:AB_2737812; PE-Cy7 mouse monoclonal anti-human CD34 (clone 581), BioLegend, catalog number 343516, RRID:AB_1877251; PerCP-Cy5.5 mouse monoclonal anti-human IgM (clone MHM-88), BioLegend, catalog number 314512, RRID:AB_2076098; PerCP-Cy5.5 mouse monoclonal anti-human CD33 (clone WM53), BioLegend, catalog number 303414, RRID:AB_2074241; and rabbit polyclonal anti-human EBF1, Cell Signaling Technology, catalog number 50752.

Results

IL-7R α deficiency impairs differentiation and expansion of early BCPs

We first compared BM BCPs of 2 patients with deleterious mutations in the IL-7R α chain (Figure 1A) with those of pediatric controls via flow cytometry (Figure 1B-E). The 2 patients with IL-7R α deficiency had relatively more CLPs and pro-B cells but less pre-B1 cells, suggesting impaired differentiation during the early phases of B lymphopoiesis and a leaky arrest at the pro-B to pre-B1 cell transition (Figure 1C-E). In line with these observations, the IL-7R α chain showed the highest expression in pro-B cells in healthy controls (Figure 1F), consistent with the accumulation of earlier BCP subsets in the patients (Figure 1C-E). As expected, IL-7R α -deficient BCPs did not express any CD127 (Figure 1F).

In order to validate our observations, we isolated CD34⁺ human hematopoietic progenitors from CB and differentiated them into BCPs in the presence or absence of IL-7, using a feeder

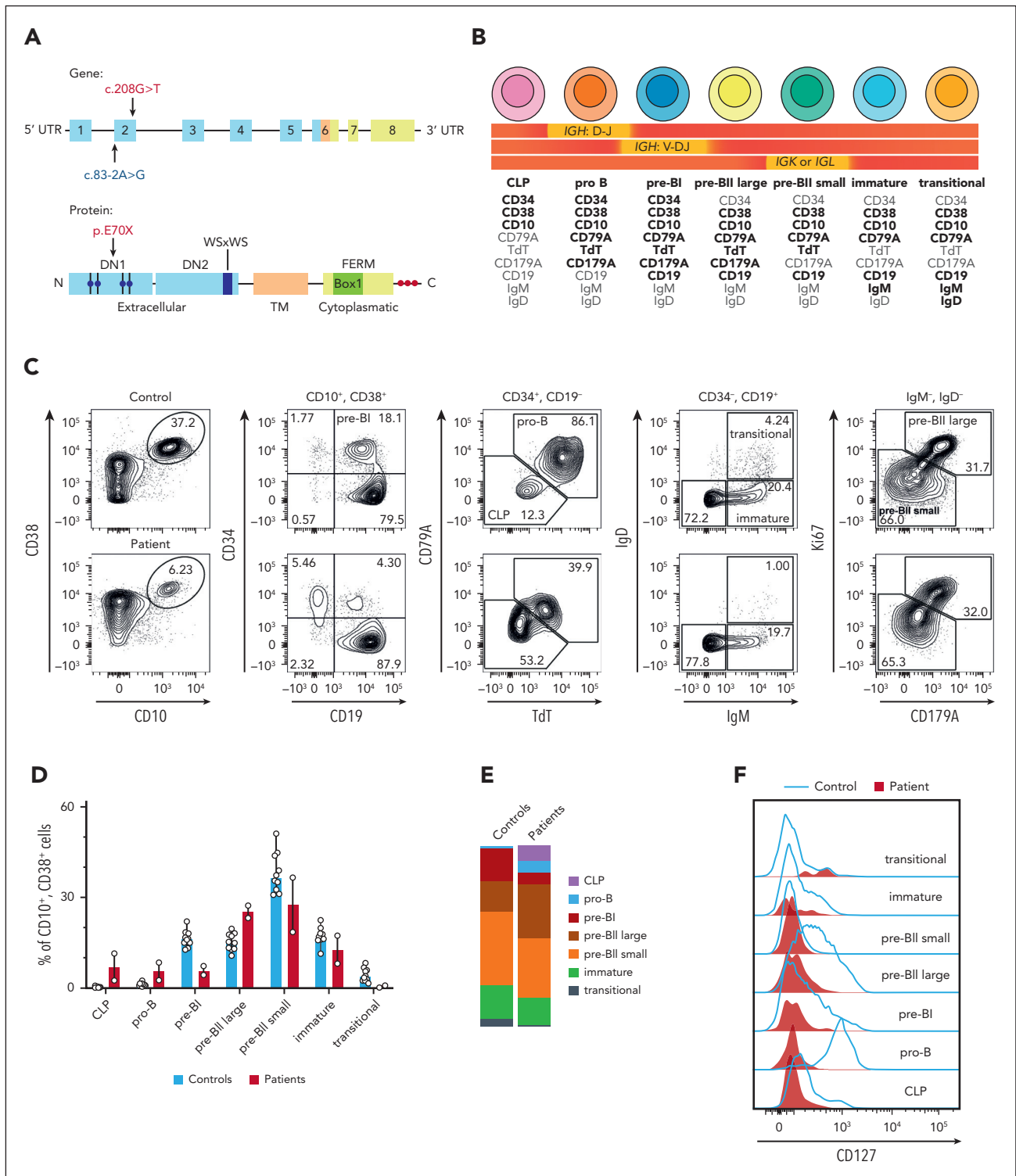


Figure 1. IL-7R α deficiency impairs the differentiation and expansion of early BCPs. (A) Overview of the IL-7R α chain with the individual domains and motifs highlighted as shown in the figure. Top graph shows the gene with exons marked as boxes; bottom graph shows the protein. Extracellular domain (blue) with fibronectin type 3-like domains DN1 and DN2 and 4 paired cysteine residues indicated by blue circles as well as WS \times WS motif; transmembrane domain (orange); intracellular domain (yellow) with four-point-one protein, ezrin, radixin, moesin (FERM) domain, BOX1 domain, and 3 tyrosine residues indicated by red circles. The mutations of the 2 patients are indicated by arrows. One patient had a homozygous premature nonsense mutation (red), whereas the other patient had a heterozygous splice acceptor site mutation (blue) and a chromosomal deletion of the other allele. (B) Markers used for the definition of the human BCP populations with the corresponding stages of V(D)J recombination. Markers that are strongly expressed by the given population are depicted in bold, whereas a lack of expression is shown in gray. (C) Flow cytometric analysis of the BCP stages in the BM, shown for 1 representative pediatric control and 1 patient. (D) Relative cell counts of the BCP stages in pediatric controls (n = 10) and the 2 patients with IL-7R α deficiency. Data show median with range. (E) Distribution of BCP stages in pediatric controls (n = 10) and the 2 patients with IL-7R α deficiency. Data show the median of each population. (F) Expression of the IL-7R α chain (CD127) on the individual human BCP subsets in the BM of a healthy pediatric control compared with a patient with IL-7R α deficiency. UTR, untranslated region.

cell-free assay³⁶ (Figure 2A; supplemental Figure 1A-B). Addition of IL-7 resulted in higher amounts of lymphocytes on day 14 with increased absolute CLP, pro-B, and pre-BI counts compared to untreated cultures (Figure 2B-C; supplemental Figure 1C). The presence of IL-7 did not change the distribution of subsets on day 14 (Figure 2D-E), suggesting a role for IL-7 in promoting the B-cell fate or inducing proliferation of early BCPs. By day 21, lymphocyte precursors had undergone substantial expansion, and IL-7-treated cultures showed a prominent increase in pre-BI cells, whereas untreated cultures mostly contained pro-B cells but also higher numbers of pre-BII large and pre-BII small cells (Figure 2B-E; supplemental Figure 1C). By day 28, pre-BI cells in the IL-7-treated cultures further expanded, whereas the untreated cultures contained a balanced mixture of early as well as late precursors, with higher numbers of pre-BII large and pre-BII small as well as immature cells without a difference in total lymphocyte counts

(Figure 2B-E; supplemental Figure 1C). Collectively, these experiments confirmed a defect during early BCP differentiation in the absence of IL-7 signaling and also revealed accelerated differentiation into later BCP subsets.

scRNA-seq of the human BCP unveils aberrant differentiation of early BCPs in patients with IL-7R α deficiency

In order to investigate the underlying molecular mechanism, we performed scRNA-seq of B-cell enriched BM of 2 healthy pediatric controls and the 2 patients with IL-7R α deficiency (Figure 3A). Analysis of the data set with the UMAP algorithm led to the identification of 15 clusters (Figure 3B-C), including 8 clusters that could be annotated as the different BCP stages based on the expression of canonical markers (Figure 3D; supplemental Figure 2A-B).

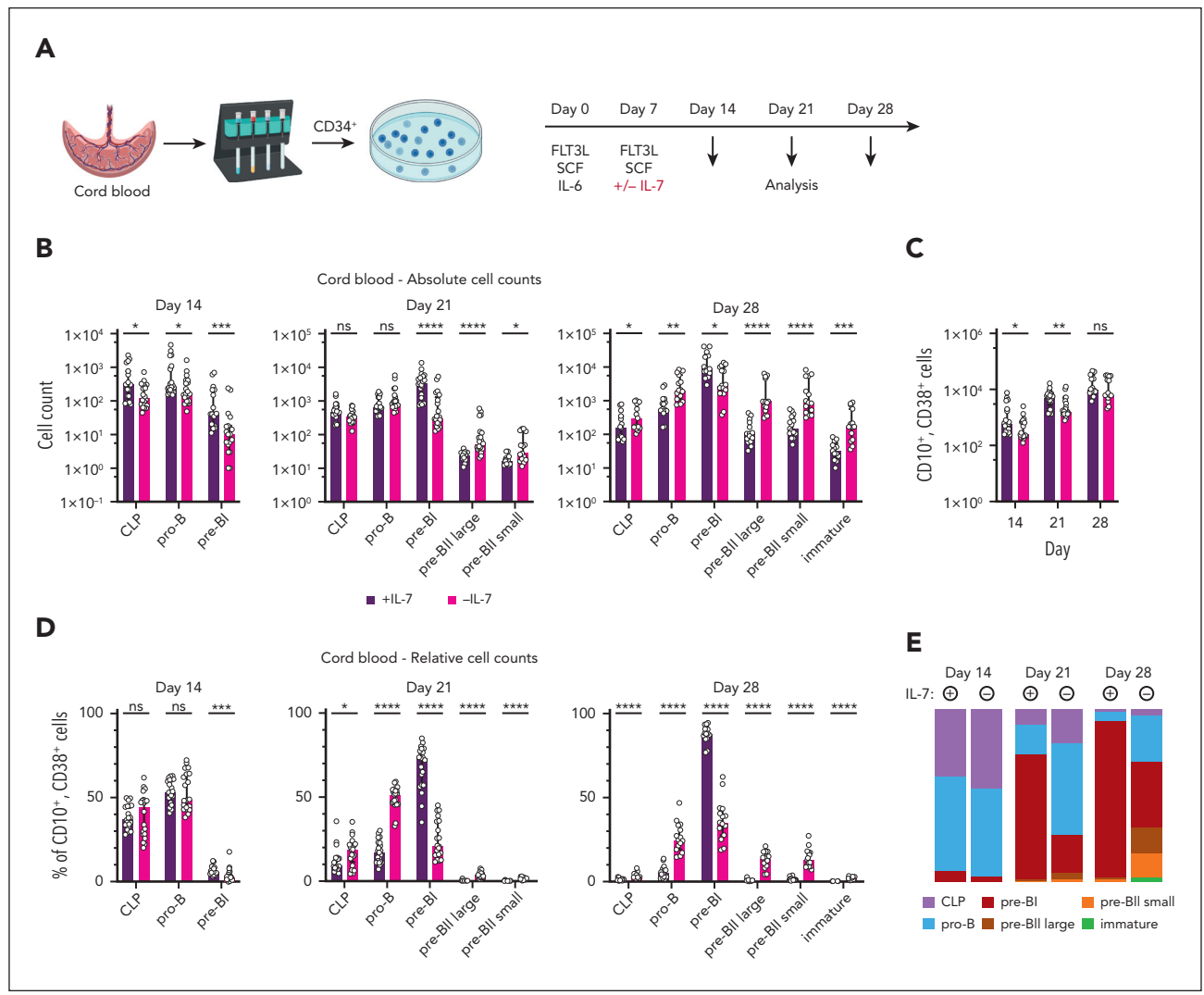


Figure 2. In vitro modeling of human B lymphopoiesis recapitulates aberrant differentiation and expansion of early BCPs in the absence of IL-7. (A) In vitro differentiation of human BCPs with CB-derived CD34⁺ hematopoietic progenitor cells. Mononuclear cells were purified via Ficoll density centrifugation and CD34⁺ progenitor cells were isolated by positive selection using magnetic-activated cell sorting. CD34⁺ cells were stimulated with FMS-like tyrosine kinase 3 ligand (FLT3L), stem cell factor (SCF), and IL-6 after isolation and restimulated with FLT3L and SCF on day 7, with IL-7 being added to the control samples. Cells were harvested on days 14, 21, and 28 after initiation of cultures for analysis. (B-E) Absolute (B-C) and relative (D) cell counts and distribution of BCP stages (E) of in vitro differentiated BCPs on days 14, 21, and 28. Data show the median, with error bars representing the interquartile range for panels B-D and the median only of each population for panel E. Statistical analysis was performed with multiple Mann-Whitney tests and corrected for multiple comparisons with the Holm-Šidák method for data shown in panels B-D (n = 7, each with 2-5 replicates). P values are denoted as follows: *P < .05; **P < .01; ***P < .001; ****P < .0001. ns, not significant.

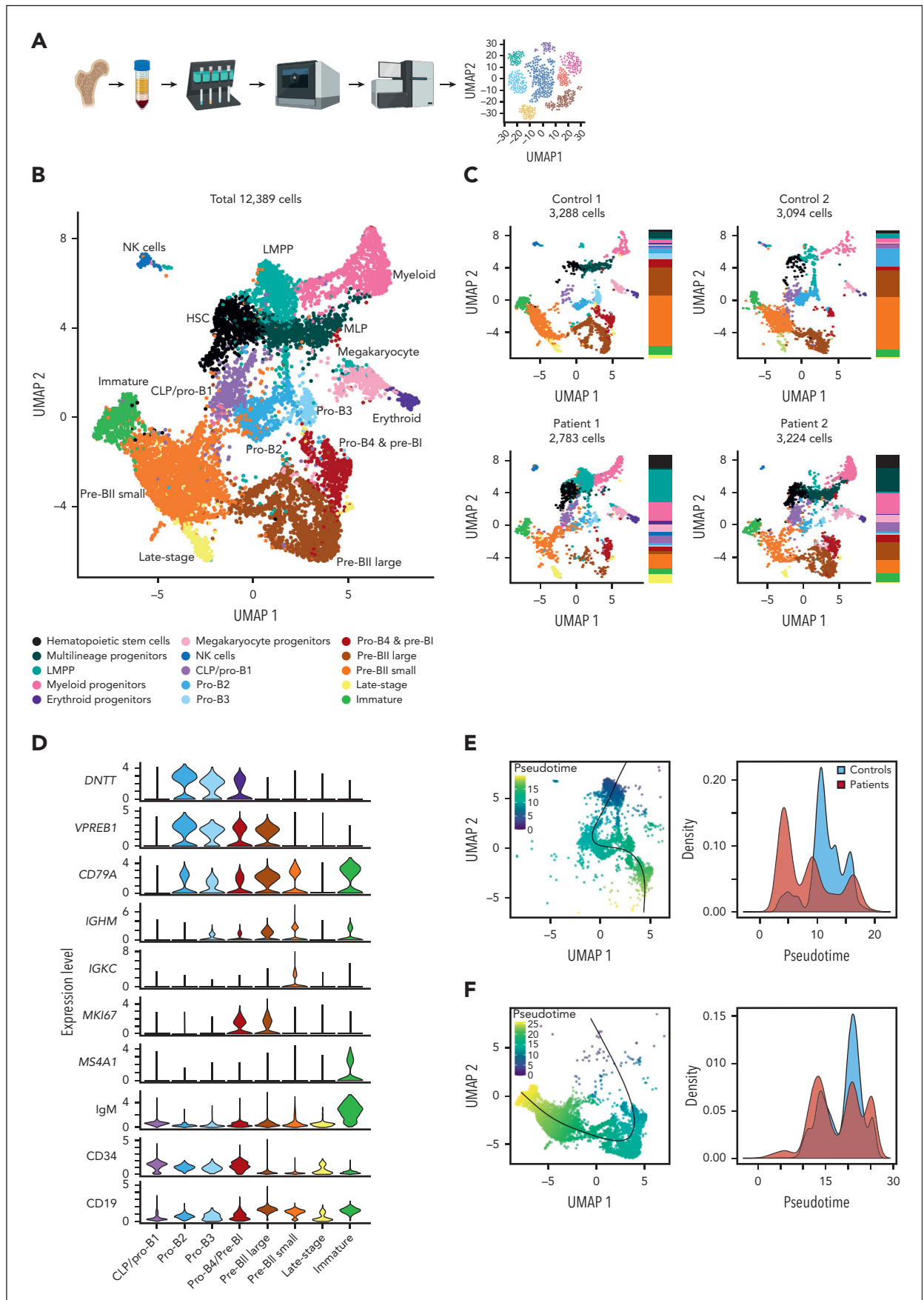


Figure 3.

Next, we split the BCP clusters into early (Figure 3E) and late BCP (Figure 3F) subsets and performed a pseudotime analysis in order to verify the cluster annotation and analyze the developmental trajectories. The distinction between these 2 subsets was based on the expression of canonical markers that allow for the differentiation of early BCPs that still undergo rearrangement of the *IGH* locus and late BCPs that proliferate upon successful rearrangement of an *IGH* allele and subsequently undergo *IGK* or *IGL* rearrangement (Figure 3D). The early BCP clusters, thus, represent LMPPs, CLPs, pro-B, and pre-BI cells (Figure 3E), whereas the late BCP clusters correspond to pre-BII large and pre-BII small as well as immature and transitional B cells (Figure 3F). Using the LMPP cluster as the starting point, the early BCP clusters showed a trend toward earlier pseudotime values in the patients (Figure 3E), reflecting the aberrant differentiation that we observed *ex vivo* and *in vitro* (Figures 1C-E and 2B-E) and suggesting impaired progression toward the B-lymphoid fate. Conversely, pseudotime analysis of the late-stage BCP clusters, using the pro-B4/pre-BI cluster as the starting point, did not show a difference in pseudotime values (Figure 3F). Thus, the scRNA-seq data confirmed the aberrant differentiation of early BCP subsets. Collectively, our results suggest impaired induction of the B-lymphoid fate as well as poor proliferation of early BCPs in the absence of IL-7. In addition, *in vitro* development in the absence of IL-7 resulted in dyssynchrony between the expression of canonical markers and the V(D)J recombination status as illustrated by the higher frequency of cytoplasmic IgM⁺ cells in untreated CLP and pro-B-cell subsets *in vitro* (supplemental Figure 3A-B), which are commonly only found in late pre-BI and pre-BII large cell subsets that have completed *IGH* recombination. Given that attenuated IL-7 signaling leads to upregulation of FoxO transcription factors and thus induction of Rag1 and Rag2 expression in mice,⁵⁰ IL-7R α chain deficiency might accelerate V(D)J recombination.

IL-7 signaling drives proliferation of early BCPs but not pre-BII large cells and has limited effects on cell death

In absence of IL-7, we observed lower absolute cell counts on days 14 and 21 *in vitro*. We therefore analyzed the expression of the proliferation marker Ki-67 in the BM of controls and patients via flow cytometry (Figure 4A). The CLPs and pro-B cells of patients showed lower expression of Ki-67, whereas all remaining subsets, including pre-BII large cells, showed nearly identical expression levels compared to controls (Figure 4A), suggesting a proliferation defect at the earliest stages of B lymphopoiesis. Analysis of the cell cycle status in the scRNA-seq data set (Figure 4B) unveiled strong differences in the distribution of cell cycle phases in the pro-B3 and pro-B4/pre-BI clusters (Figure 4C). Although most control cells were either in the S or G2/M phase, the majority of patient cells in the pro-B3 cluster were not cycling, and 18% of the cells in the pro-B4/pre-BI

cluster were still in the G1 phase (Figure 4C). Of note, the distribution of cycling and noncycling cells in the pre-BII large cluster were nearly identical (Figure 4C).

The analysis of genes that correlate with proliferation in the individual clusters unveiled higher expression of proliferation markers in the control pro-B3 and pro-B4/pre-BI clusters compared to the corresponding patient clusters (Figure 4D). Of note, these genes were similarly expressed in the pre-BII large cluster between controls and patients (Figure 4D), confirming the lack of a strong proliferative defect in the subset of cells that have successfully rearranged the *IGH* locus. In addition, GSEA confirmed the difference in proliferation between control and patient cells in the pro-B4/pre-B cluster (Figure 4E).

Given the known role of cyclin D3 in inducing proliferation of early BCPs in response to IL-7R signaling in mice,^{9,10} we analyzed the expression of the *CCND3* gene in the early BCP clusters (Figure 4F). We observed higher expression of *CCND3* in the pro-B3 and pro-B4/pre-BI control clusters compared to the corresponding patient clusters, thus suggesting a central role for cyclin D3 in regulating proliferation and expansion of the early BCP pool in response to IL-7R signaling in humans as well.

In order to validate our findings, we investigated the expression of Ki-67 in the *in vitro* differentiated CB-derived BCPs 1 week after stimulation with IL-7 (Figure 4G). Consistent with the findings of the flow cytometry and scRNA-seq data, the frequency of Ki-67-expressing cells was higher in the IL-7-stimulated cells (Figure 4G). Stimulation of CD34⁺-enriched, BM-derived hematopoietic progenitors and BCPs confirmed these findings (Figure 4H; supplemental Figure 1D), thus excluding a potential age-related difference in the response to IL-7.

Although IL-7R signaling plays a prominent role in preventing apoptosis of early BCPs in mice,¹³⁻¹⁶ we found no differences in phosphatidylserine levels as measured by Annexin V staining of the individual BCP subsets of the 2 patients and healthy controls (supplemental Figure 4A). Similarly, we did not observe a difference in cell death between IL-7-treated and untreated cultures *in vitro* after staining with the live-dead cell marker Zombie (supplemental Figure 4B-C). However, GSEA of the pro-B3 and pro-B4/pre-BI clusters unveiled a clear apoptosis and p53 signaling signature in the patient cells (supplemental Figure 4D-E). The discrepancy between the flow cytometric staining for phosphatidylserine and the GSEA might be due to the rapid clearance of preapoptotic cells *in vivo*. In summary, these findings confirm a minor role for IL-7R signaling in the prevention of apoptosis *in vivo* and suggest that additional signaling pathways safeguard survival of early BCPs in humans.

Figure 3. scRNA-seq recapitulates aberrant differentiation of early BCPs in patients with IL-7R α deficiency. (A) Preparation of the scRNA-seq data set. Mononuclear cells of BM samples of 2 healthy pediatric donors and 2 patients with IL-7R α deficiency were isolated via Ficoll density centrifugation, depleted of dead cells, stained with CITE-seq antibodies, and enriched for BCPs using magnetic-activated cell sorting before preparing the single-cell library according to the 10x Chromium protocol, followed by sequencing using Illumina technology. (B) UMAP plot showing the distribution of the individual clusters of the entire data set of patient and control samples. (C) Individual UMAP plots showing the clusters and their distribution in the adjacent panel for each control and patient. Color coding is identical to that in panel B. (D) Violin plots showing the expression of the B-cell markers used for the annotation of the individual B-cell clusters. Bottom 3 panels represent CITE-seq markers. (E-F) Pseudotime analysis for the early (E) and late (F) BCP subsets. Left panels in panels C-E-F show pseudotime calculated as described in "Methods" and plotted on the UMAP of the respective data set; right panels show comparison of pseudotime values for controls vs patients. Black lines in the left plots in panels E-F denote the trajectories.

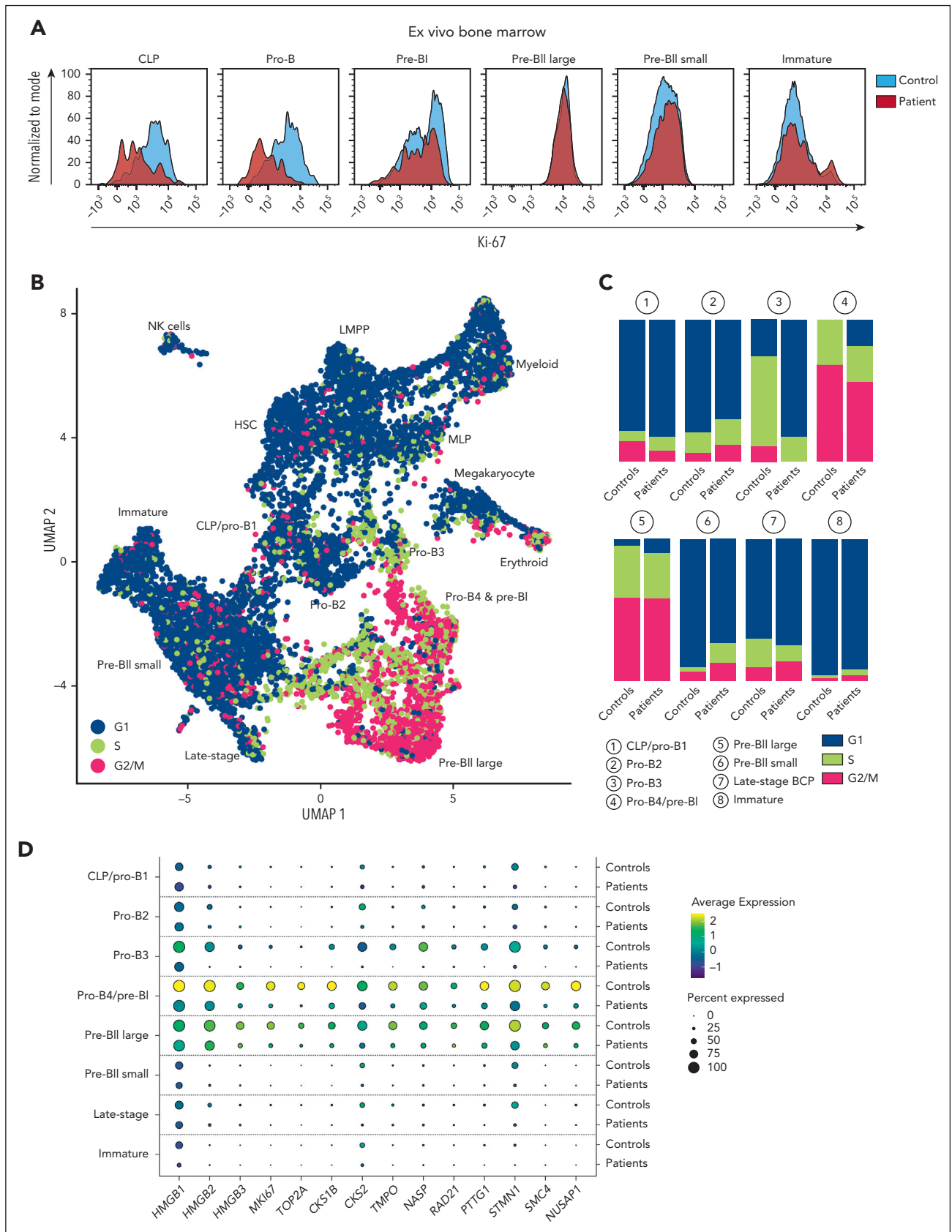


Figure 4. IL-7 signaling induces proliferation of early BCP but does not profoundly affect proliferation of pre-BII large cells. (A) Flow cytometric quantification of Ki-67 expression in individual BM BCP populations in controls vs patients, shown for 1 representative control and 1 patient. (B) Cells were assigned to the different cell cycle phases as described in "Methods." UMAP plot of the entire combined data set of controls and patients, showing the cell cycle phase of each cell (blue: G1; green: S phase; and pink: G2/M phase). (C) Distribution of cell cycle phases per cluster shown for controls vs patients. Bars indicate percentages per cluster.

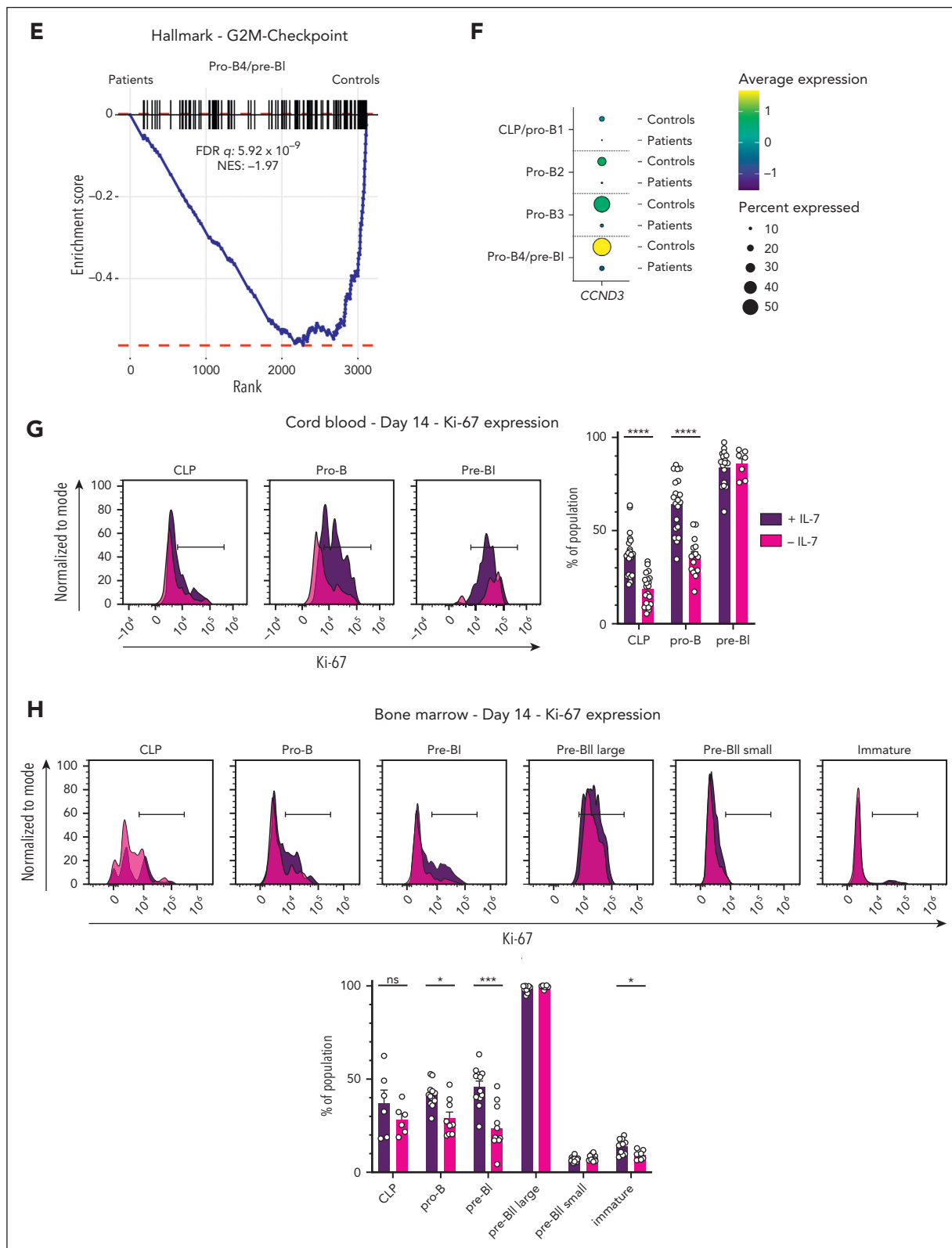


Figure 4 (continued) (D) Dot plot showing expression of proliferation markers for individual clusters in controls vs patients. (E) GSEA analysis with the G2M hallmark gene set performed for the pro-B4/pre-B1 cluster with the differentially expressed genes between patients and controls, showing enrichment of the gene set in the controls. (F) Dot plot showing expression of *CCND3* in early BCP clusters in controls vs patients. (G-H) Flow cytometric quantification of Ki-67 expression in individual BCP populations in IL-7 stimulated vs unstimulated CB (G) and BM (H) cultures. The black bar denotes gate for positive cells. Bar graphs show mean with error bars representing standard error of the mean. Statistical analysis was performed with multiple unpaired t tests and corrected for multiple comparisons with the Holm-Šidák method. All replicates are shown (CB: $n = 7$, each with 2-5 replicates; BM: $n = 3$, each with 3-6 replicates). P values are denoted as follows: * $P < .05$; *** $P < .001$; **** $P < .0001$.

Collectively, our data proves that IL-7R signaling induces proliferation of early BCPs without profoundly affecting proliferation of pre-BII large cells. Moreover, IL-7 has a limited role in the prevention of programmed cell death in early BCPs.

IL-7 signaling enhances expression of EBF1 and PAX5 in early BCPs

Next, we investigated the expression of *EBF1* and *PAX5* across the pseudotime of the early BCP subset and observed higher expression of both transcription factors in the controls compared to the patients (Figure 5A; supplemental Figure 5A). In the controls, the expression of both transcription factors coincided with the expression of *BACH2* (Figure 5A; supplemental Figure 5A), which has been associated with the suppression of myeloid genes as well as enhanced expression of *Ebf1* and *Pax5* in early lymphoid progenitors in mice.⁵¹ In line with the higher expression of *EBF1* and *PAX5* in the control cells, we also observed higher expression of the genes *CD79A*, *CD79B*, *VPREB1*, and *IGLL1*, which all encode essential components of the (pre-)BCR and are known target genes of *Ebf1* and *Pax5* in mice (Figure 5B).^{52,53} The higher expression of the *EBF1*-target genes *PAX5* and *CD79A* as well as that of the *PAX5*-target gene *CD19* in the control cells was also confirmed at the protein level via flow cytometry (Figure 5C).

Given the essential role of *Ebf1* and *Pax5* in shutting down alternative cell lineages, we investigated the expression of myeloid genes in the early BCP clusters (Figure 5D). We observed higher expression of several genes that were enriched in the myeloid progenitor cluster (supplemental Figure 5B) in the early BCPs of the patients as well as concomitantly lower expression of lymphoid and, particularly, B-lymphoid genes (Figure 5D). Given these strong gene expression differences, the patient CLP/pro-B1 cluster also clustered separately when we performed unsupervised clustering of the earliest BCP clusters, suggesting impaired specification of the B-lymphoid transcriptome due to low *EBF1* and *PAX5* expression (Figure 5D). Although we observed more myeloid progenitors in the patient scRNA-seq data set (Figure 3C), the total number of myeloid cells in the in vitro experiment with CB-derived hematopoietic progenitors did not differ between the IL-7-treated and -untreated conditions (supplemental Figure 5C). However, it is important to note that the experimental conditions did not favor myelopoiesis. Furthermore, the higher frequency of myeloid progenitors in the patients might also reflect emergency myelopoiesis in response to frequent infections. Recent studies have shown that the lymphotoxin- β receptor (TNFRSF3) signaling pathway reduces IL-7 production in the BM niche⁵⁴ and that the lymphotoxin- β receptor ligand lymphotoxin- $\alpha 1\beta 2$, which is expressed by B-lineage cells, downregulates IL-7 secretion to promote emergency myelopoiesis while repressing lymphopoiesis in systemic inflammation.⁵⁵ We observed higher expression of *LTB* (encoding lymphotoxin- $\beta 2$) in several early BCP subsets but not in immature B cells of the controls compared to the patients (supplemental Figure 5D), whereas the expression of *LTA* was near-absent in the data set. Yet, lymphotoxin- $\alpha 1\beta 2$ is mostly secreted by mature B cells in mice,⁵⁵ which are not present in the BCP scRNA-seq data set but still found in nearly normal numbers in patients with IL-7R α deficiency.

In order to validate our findings, we analyzed the expression of *EBF1* and *PAX5* 7 days after stimulation with IL-7 in vitro (Figure 5E-F; supplemental Figure 6A-D). Both *EBF1* and *PAX5* expression were significantly higher in BCPs upon IL-7 stimulation in BM and CB cultures (Figure 5E-F; supplemental Figure 6A-D). Consistent with the increased expression of *EBF1* and *PAX5* in IL-7-stimulated cells, we also observed higher expression of *CD79A* and *CD19* in IL-7-treated cultures (Figure 5G-H; supplemental Figure 6E-F), confirming that IL-7 also indirectly affects the expression of *EBF1*- and *PAX5*-target genes. Thus, our data confirm that IL-7 signaling enhances the expression of *EBF1* and *PAX5* in human BCPs.

In addition, we detected higher expression of the genes *CD74* and *CXCR4* in the scRNA-seq data across the pseudotime of the early BCP subset in the controls (Figure 5A). Besides its role in generating the invariant chain for antigen presentation,^{56,57} *CD74* functions as the receptor for macrophage migration inhibitory factor (MIF)⁵⁸ and uses *CXCR4* as 1 of its coreceptors.⁵⁹ In mice, *CD74* has multiple important functions in B lymphopoiesis, such as proliferation, survival, maturation, and migration,⁵⁹⁻⁶² and *CXCR4* also functions as the receptor for the chemokine *CXCL12*, which is critical for directing early progenitors into the appropriate BM niche.^{1,63} The reduced expression of both genes in patient early BCPs could therefore also account for part of the phenotype.

Higher expression of AP-1 transcription factors in IL-7R α -deficient BCPs

Whereas IL-7 enhanced the expression of the transcription factors *BACH2*, *EBF1*, and *PAX5* in early BCPs in vivo and in vitro, we observed lower expression of several activator protein 1 (AP-1) transcription factors in BCPs of healthy controls compared to BCPs of the patients (Figure 5I; supplemental Figure 7A). AP-1 transcription factors are ubiquitously expressed dimeric basic region leucine zipper transcription factors that bind to common AP-1 binding sites and are formed by the heterodimerization of Jun and Fos family transcription factors.⁶⁴ AP-1 transcription factors have been implicated in a wide array of cellular functions, such as proliferation, apoptosis, and differentiation and assume multiple roles in the development of progenitors into mature blood cells across multiple hematopoietic lineages,⁶⁵ including B lymphocytes.⁶⁶ Although the expression of both JUN and FOS family members in progenitor clusters was similar between controls and patients (Figure 5I; supplemental Figure 7A), the patients' early and late BCP clusters showed consistently higher expression of *JUN*, *JUNB*, *JUND*, *FOS*, and *FOSB* (Figure 5I). Previous work has shown that expression of the IL-7R α chain and TdT increases in BCPs during the transition from fetal to pediatric hematopoiesis.²⁷ Given that AP-1 transcription factors have been suggested to negatively regulate TdT expression,⁶⁷ we reanalyzed the published gene expression data, which unveiled higher expression of both JUN and FOS family members in both fetal pro-B and pre-BI cells compared to their pediatric counterparts (supplemental Figure 7B). Collectively, these observations suggest that upregulation of IL-7R expression coincides with downregulation of AP-1 transcription factors during the transition from fetal to pediatric B lymphopoiesis and that IL-7R α deficiency impairs the downregulation of both JUN and FOS family members in BCPs.

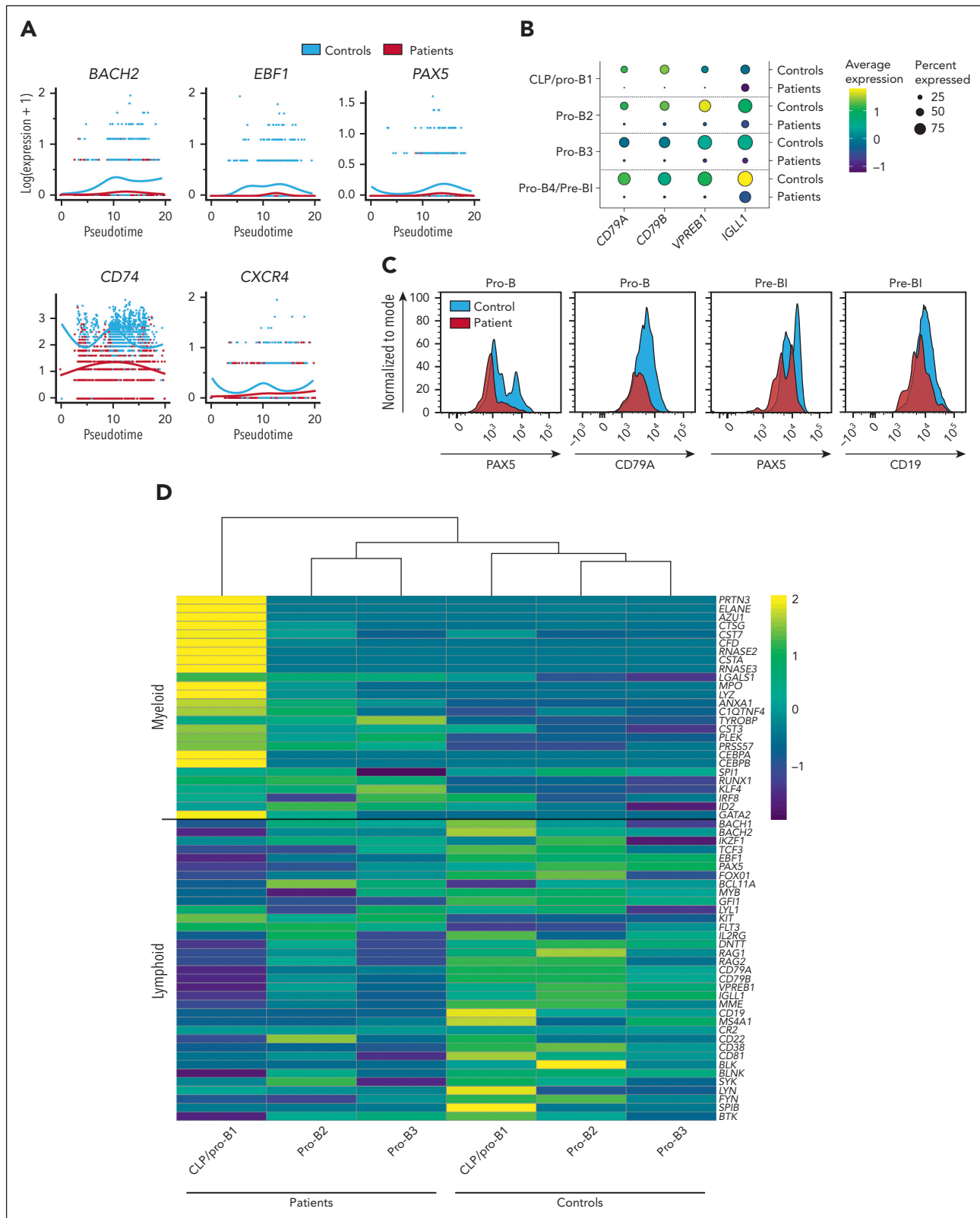


Figure 5. IL-7R α signaling stimulates the B-lymphoid fate and represses AP-1 transcription factors. (A) Expression of *BACH2*, *EBF1*, *PAX5*, *CD74*, and *CXCR4* plotted across the pseudotime of the early BCP subset as shown for controls and patients. (B) Dot plots showing expression of the *EBF1* and *PAX5* target genes *CD79A*, *CD79B*, *VPREB1*, and *IGLL1* in early BCP clusters in controls vs patients. (C) Flow cytometric quantification of *PAX5*, *CD79A*, and *CD19* expression in indicated BCP populations in the BM of controls and patients. (D) Heatmap showing expression of myeloid and lymphoid genes in early BCP clusters with unsupervised clustering. (E-H) Flow cytometric quantification of *EBF1* (E), *PAX5* (F), cytoplasmic *CD79A* (G), and *CD19* (H) expression in individual BCP populations in IL-7-stimulated vs unstimulated BM cultures at day 14. Representative histograms are shown in supplemental Figure 6. Bar graphs show the median with interquartile range (E,G-H) or mean with standard error of the mean (F).

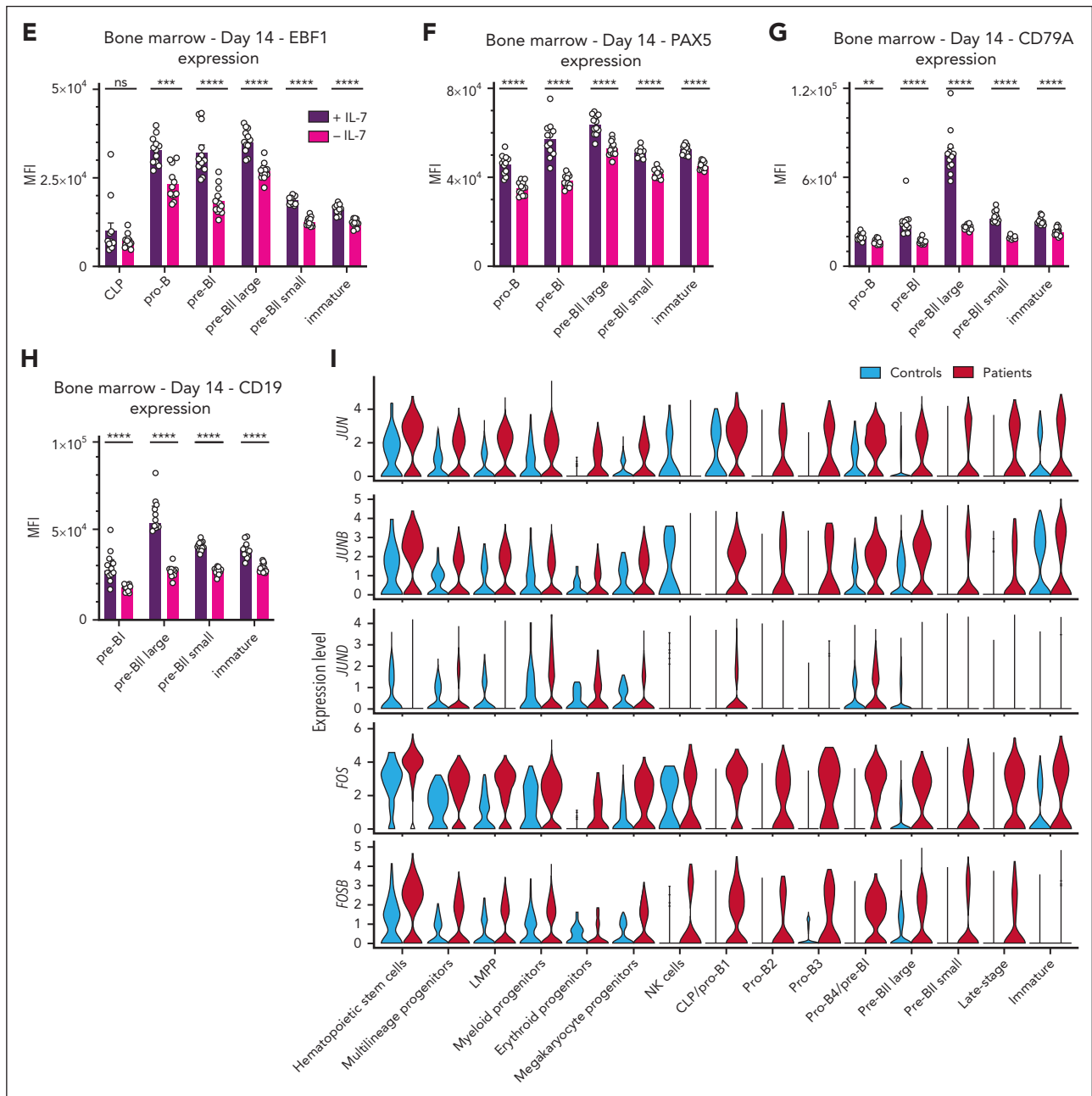


Figure 5 (continued) Statistical analysis was performed with multiple Mann-Whitney tests (E,G-H) or unpaired t tests (F) and corrected for multiple comparisons with the Holm-Šidák method. Data collected from 3 experiments with 3 different BM donors. All replicates are shown (n = 3 BM samples, each with 3 or 6 replicates). (I) Violin plots showing expression of JUN and FOS family members across all clusters in patients vs controls. P values are denoted as follows: **P < .01; ***P < .001; ****P < .0001.

IL-7R α deficiency does not have a major effect on N-nucleotide addition but increases IGH repertoire clonality

Consistent with previous experiments that have suggested a role for IL-7R signaling in inducing expression of TdT in pro-B and pre-BI cells,²⁷ we observed higher expression of TdT in pro-B and pre-BI cells of controls compared with those of patients (supplemental Figure 8A). In contrast, TdT expression was marginally higher in the IL-7–treated cultures with human BM but only in pro-B and not in pre-BI cells (supplemental Figure 8B). However, it is important to note that CD34-enrichment of BM-derived hematopoietic progenitors also

leads to the isolation of pro-B and pre-BI cells that have already been exposed to IL-7 in vivo, which might still affect TdT expression levels after expansion and stimulation in vitro (supplemental Figure 8B). In order to validate the effect of IL-7 on N-nucleotide addition, we sequenced IGH junctions of naive mature B cells isolated from peripheral blood of patients and healthy, age-matched infant controls as well as additional patients with T⁻ B⁺ SCID with deleterious mutations in the genes encoding for JAK3 or the γ chain, which are also part of the IL-7R complex (supplemental Figure 8C). The junctions of both productive and unproductive sequences showed no major differences, neither with regard to the number of N-nucleotides

nor to the number of deleted nucleotides, thus resulting in similar CDR3 lengths (supplemental Figure 8C). We therefore conclude that the effect of IL-7 on TdT net activity is likely negligible, given the similar N-nucleotide numbers in patients with SCID and age-matched controls.

IL-7 signaling has also been implicated in *IGH* repertoire diversification both at the D_H -to- J_H and V_H -to- DJ_H stages of

recombination in mice.¹⁷ However, we observed a similar distribution of V, D, and J genes without skewing toward 3' V_H gene usage in patients and controls (Figure 6A-B). Of note, our *IGH* repertoire analysis was performed with naive mature B cells that have undergone selection and, thus, does not fully reflect the V, D, and J gene selection during V(D)J recombination. Importantly, repertoire clonality was increased in the patients compared to age-matched controls (Figure 6C), suggesting an

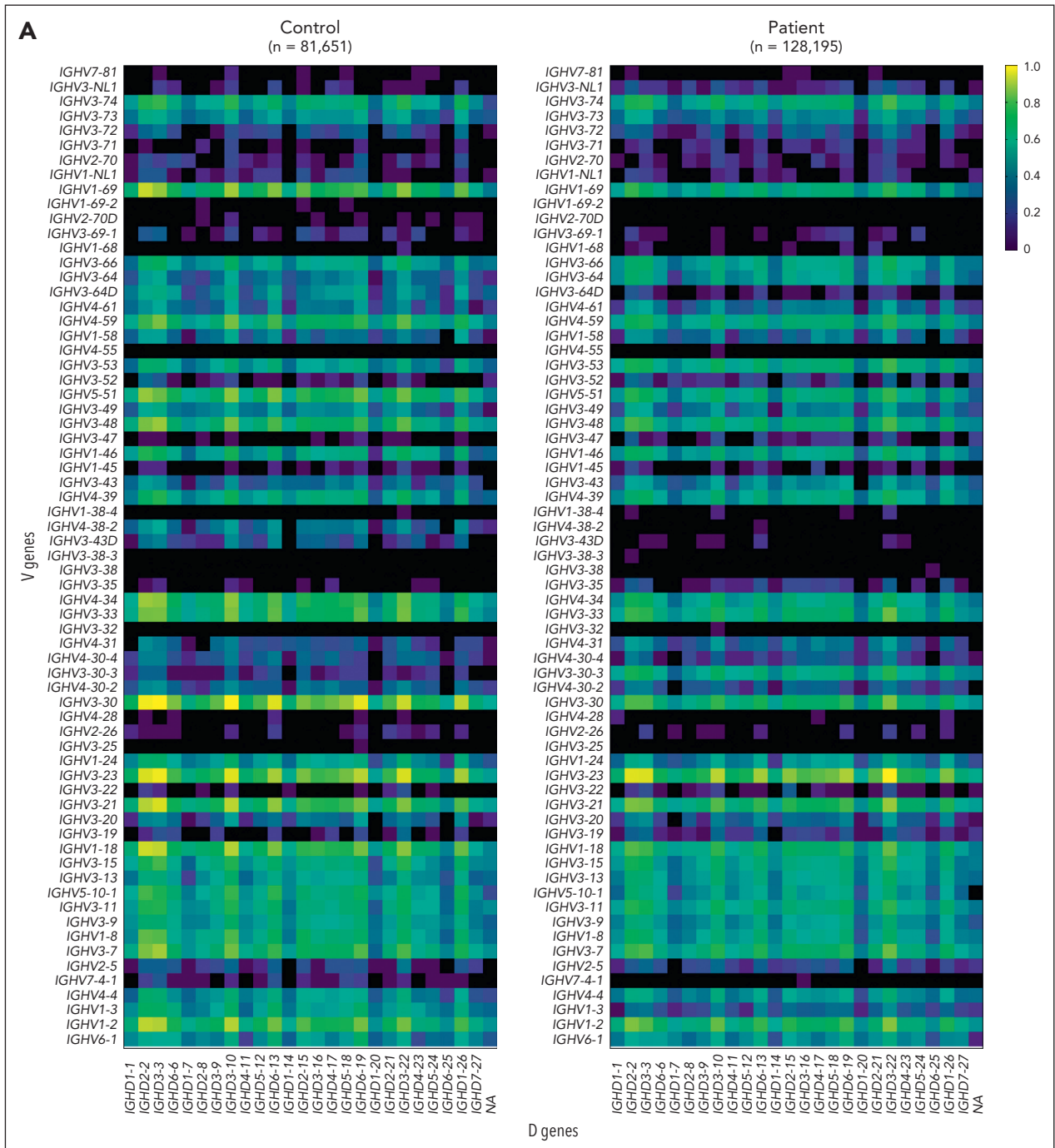


Figure 6. IL-7R α deficiency increases *IGH* repertoire clonality. (A-B) Heatmaps showing distribution of V and D genes (A) and D and J genes (B) in *IGH* repertoire of a representative control and patient. Data show relative values determined by dividing the log of the frequency count of a given gene by the maximum, in order to normalize between 0 and 1. The amount of sequences is indicated above each heatmap. (C) Clonality score of *IGH* repertoire in healthy, age-matched controls (n = 3) and the patients with IL-7R α deficiency (n = 2) as defined by Boyd et al.⁴⁹ Data shown as median with range.

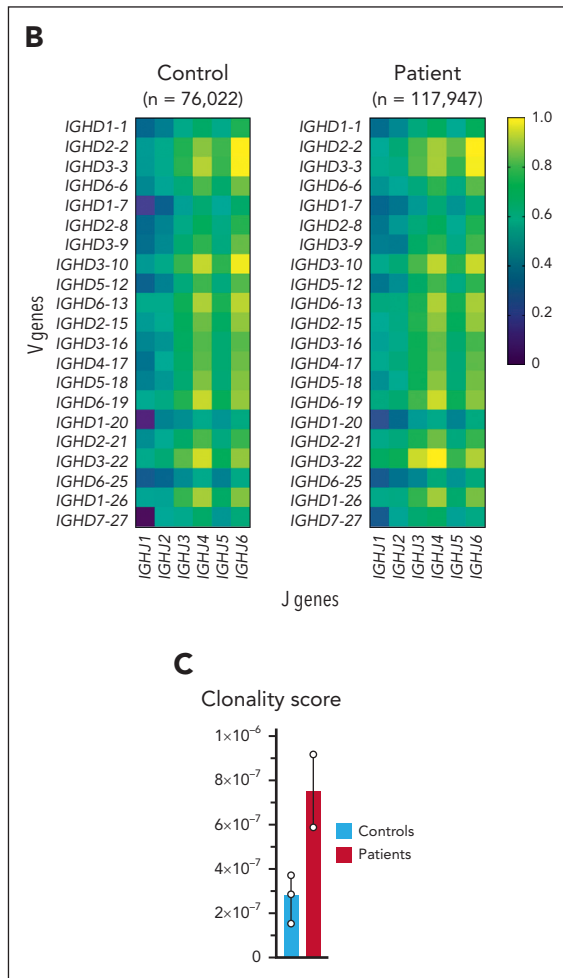


Figure 6 (continued)

effect of the aberrant early BCP differentiation and expansion on the naive mature *IGH* repertoire.

Discussion

Here, we demonstrate that IL-7 signaling fulfills a crucial role in human B lymphopoiesis by inducing proliferation of the early BCP pool and enhancing *EBF1* and *PAX5* expression, which induce B-cell specification and commitment of early lymphoid progenitors in mice.^{68,69} *EBF1* and *PAX5* expression was reduced but not absent in patient early BCPs or cultures that were not supplemented with IL-7, suggesting that IL-7 acts in concert with other transcription factors, such as *E2A*,^{70,71} similar to its role in mouse B-cell development.^{6,8,72} In addition, IL-7 enhanced expansion of early human BCPs but neither had a strong effect on the proliferation of pre-BII large cells nor on the survival of BCPs, thus unveiling 2 important differences between human and murine B lymphopoiesis. Collectively, these findings may explain the discrepancy between IL-7R α -deficient mice and SCID patients.

Besides the upregulation of cyclin D3, early BCPs of controls showed upregulation of the transcription factor *BACH2*, the MIF-receptor *CD74*, and the chemokine receptor *CXCR4*, which also functions as a coreceptor for *CD74*.⁷³ Interestingly, the

expression of all 3 genes was also upregulated in murine pre-B cells that were proliferating independently of the pre-BCR and connected to IL-7R signaling.⁷⁴ In mice, *CD74* has previously been associated with proliferation, survival, maturation, and migration in B cells,⁵⁹⁻⁶² suggesting an additional signaling pathway that is activated by IL-7 to induce proliferation in humans. Besides its role in MIF signaling, *CXCR4* functions as the receptor for the chemokine *CXCL12*, which is critical for B lymphopoiesis because it guides progenitors into the niche, where they are exposed to high levels of IL-7,^{1,63} which could induce a self-amplifying loop that is driven by the IL-7R.

Although specification and commitment of lymphoid progenitors to the B-cell fate is driven by *Ebf1* and *Pax5*,^{70,71} which shut down alternative cell lineage options such as the myeloid fate, *Bach2* has also been implicated in downregulating expression of myeloid genes while concomitantly enhancing expression of *Ebf1* and *Pax5* in early progenitors in mice.⁵¹ Consistent with this observation, *BACH2* expression coincided with the upregulation of *EBF1* and *PAX5* in controls. Compared with controls, early BCP of patients expressed high levels of myeloid-specific genes as well as lower levels of *EBF1* and *PAX5* and their target genes. Although *BACH2* induction has not been associated with IL-7 signaling in mice, it could be a missing link between IL-7 and *EBF1* and *PAX5* induction, particularly given the controversy regarding functional *STAT5* binding sites in the regulatory elements of the *Ebf1* and *Pax5* genes.⁷⁵⁻⁷⁷

Our data suggest an interplay between the IL-7R, *BACH2*, and AP-1 transcription factors. As expression of the IL-7R α chain increases during the transition from fetal to pediatric hematopoiesis, both *JUN* and *FOS* family members are down-regulated.²⁷ In IL-7R α -deficient BCPs, we also detected lower expression of *BACH2*, which has previously been shown to regulate CD8⁺ T-cell differentiation by controlling access of AP-1 transcription factors to enhancers.⁷⁸ IL-7R signaling might, thus, antagonize *JUN* and *FOS* transcription factors via a dual mechanism by repressing their expression and by restricting their access to enhancers via *BACH2*. However, the functional consequences of this process are unclear. AP-1 transcription factors have been broadly implicated in priming enhancer repertoires during development⁷⁹ and could, for instance, support the expansion of hematopoietic progenitors during fetal hematopoiesis.

Consistent with the dual function of IL-7 during the early phase of human B-cell development, the clonality of the patients' *IGH* repertoire was increased. Given that *IGH* repertoire diversity is based upon a large and diverse early BCP pool, it is likely dependent on IL-7-driven expansion. As early progenitors underwent rapid *IGH* recombination while concomitantly showing impaired proliferation in the absence of IL-7R signaling in vitro, the patients likely generated a smaller pool of cells with diverse *IGH* alleles. Although we did not observe a gross difference in N-nucleotide addition, we confirmed a role for IL-7 signaling in enhancing TdT expression, potentially by repressing AP-1 expression and activity.⁶⁷ Of note, the repertoire analysis was performed with naive mature B cells of age-matched healthy controls because all patients with SCID receive HSCT within the first year of life. It is, thus, unknown how a lack of IL-7 signaling would affect repertoire diversity at an older age. Importantly, this question also applies to patients

with SCID with mutations in JAK3 or the γ chain, given that both proteins are part of the IL-7R complex.

Thus far, HSCT remains the only curative option for SCID. Although there used to be no consensus regarding the application of a chemotherapeutic conditioning regime prior to HSCT of patients with IL-7R α -deficient SCID,^{33,34} frequently assuming that autologous BCPs do not have to be eradicated in order to acquire full humoral immunocompetence after transplantation, recent guidelines recommend conditioning in the majority of cases.⁸⁰ Unfortunately, large-scale studies that assess the immunocompetence of patients who are conditioned vs those who are not are currently lacking, and the long-term impact of autologous IL-7R α -deficient BCPs on humoral immunity is unresolved.

Our data prove a crucial role for IL-7 in promoting the B-lymphoid fate by enhancing BACH2, EBF1, and PAX5 expression and inducing proliferation of early BCPs up to the pre-BII large stage. In contrast to its role in murine B-cell development, IL-7R signaling has a minor role in the prevention of apoptosis. These thus-far unknown similarities and differences between human and murine B lymphopoiesis may explain the discrepancy in B-cell numbers between mice and men and raise important concerns regarding the immunocompetence of patients with IL-7R α deficiency with autologous BCPs after HSCT.

Acknowledgments

The authors are grateful to the patients and their families for their cooperation and participation in the study. The authors express their gratitude to the children and their parents as well as the adult patients who donated BM for our study. All illustrations were created with [BioRender.com](https://www.biorender.com).

This work was supported by the Stichting Sophia Kinderziekenhuis Fonds (S15-07) and a grant from the 10X Genomics Grant Program LUMC (M.v.d.B.). M.R. was funded by the Deutsche Forschungsgemeinschaft (German Research Foundation, project number 468499998).

Authorship

Contribution: F.M.P.K., M.v.d.B., and M.R. conceived and designed the study; F.M.P.K. and I.P.-K. performed the flow cytometric analysis of the human BM samples and the *IGH* repertoire analysis; I.P.-K. generated the scRNA-seq data set; F.M.P.K., M.d.G., R.M., I.K., P.A.v.S., and S.K. analyzed the scRNA-seq data; I.J. and J.K. performed and analyzed the in vitro experiments; A.S., T.W.K., A.C.L., L.K., and M.E. provided

human BM and CB samples; M.R. and M.v.d.B. supervised the research; F.M.P.K., I.J., M.R., and M.v.d.B. wrote the manuscript; and all authors discussed the data and the manuscript.

Conflict-of-interest disclosure: The authors declare no competing financial interests.

ORCID profiles: F.M.P.K., 0000-0002-0335-2859; R.M., 0000-0002-5266-0639; M.d.G., 0000-0003-2868-0127; J.K., 0000-0002-4055-525X; T.W.K., 0000-0002-7421-3370; M.E., 0000-0002-7261-1447; S.K., 0000-0001-9189-0640; M.R., 0000-0002-5153-6089; M.v.d.B., 0000-0002-1510-3104.

Correspondence: Mirjam van der Burg, Department of Pediatrics, Laboratory for Pediatric Immunology, Leiden University Medical Center, Albinusdreef 2, 2333 ZA Leiden, The Netherlands; email: m.van_der_burg@lumc.nl; and Marta Rizzi, Department of Rheumatology and Clinical Immunology, University Medical Center Freiburg, Breisacherstr 115, 79106 Freiburg, Germany; email: marta.rizzi@uniklinik-freiburg.de.

Footnotes

Submitted 26 January 2023; accepted 5 June 2023; prepublished online on *Blood* First Edition 27 June 2023. <https://doi.org/10.1182/blood.2023019721>.

*F.M.P.K. and I.J. contributed equally to this study.

†R.M. and M.d.G. contributed equally to this study.

‡M.R. and M.v.d.B. contributed equally to this study.

The scRNA-seq data are deposited in the Gene Expression Omnibus database (accession number GSE214693).

IGH repertoire sequencing data are available at the NCBI Sequencing Read Archive (BioProject number PRJNA880632).

Data are available on request from the corresponding authors, Mirjam van der Burg (m.van_der_burg@lumc.nl) and Marta Rizzi (marta.rizzi@uniklinik-freiburg.de).

The online version of this article contains a data supplement.

There is a [Blood Commentary](#) on this article in this issue.

The publication costs of this article were defrayed in part by page charge payment. Therefore, and solely to indicate this fact, this article is hereby marked "advertisement" in accordance with 18 USC section 1734.

REFERENCES

- Cordeiro Gomes A, Hara T, Lim VY, et al. Hematopoietic stem cell niches produce lineage-instructive signals to control multipotent progenitor differentiation. *Immunity*. 2016;45(6):1219-1231.
- Grabstein KH, Waldschmidt TJ, Finkelman FD, et al. Inhibition of murine B and T lymphopoiesis in vivo by an anti-interleukin 7 monoclonal antibody. *J Exp Med*. 1993;178(1):257-264.
- Peschon JJ, Morrissey PJ, Grabstein KH, et al. Early lymphocyte expansion is severely impaired in interleukin 7 receptor-deficient mice. *J Exp Med*. 1994;180(5):1955-1960.
- von Freeden-Jeffry U, Vieira P, Lucian LA, McNeil T, Burdach SE, Murray R. Lymphopenia in interleukin (IL)-7 gene-deleted mice identifies IL-7 as a nonredundant cytokine. *J Exp Med*. 1995; 181(4):1519-1526.
- Miller JP, Izon D, DeMuth W, Gerstein R, Bhandoola A, Allman D. The earliest step in B lineage differentiation from common lymphoid progenitors is critically dependent upon interleukin 7. *J Exp Med*. 2002;196(5): 705-711.
- Kikuchi K, Lai AY, Hsu C-L, Kondo M. IL-7 receptor signaling is necessary for stage transition in adult B cell development through up-regulation of EBF. *J Exp Med*. 2005;201(8):1197-1203.
- Clark MR, Mandal M, Ochiai K, Singh H. Orchestrating B cell lymphopoiesis through interplay of IL-7 receptor and pre-B cell receptor signalling. *Nat Rev Immunol*. 2014; 14(2):69-80.
- Tsapogas P, Zandi S, Åhsberg J, et al. IL-7 mediates Ebf-1-dependent lineage restriction in early lymphoid progenitors. *Blood*. 2011; 118(5):1283-1290.
- Cooper AB, Sawai CM, Sicinska E, et al. A unique function for cyclin D3 in early B cell development. *Nat Immunol*. 2006;7(5): 489-497.
- Mandal M, Powers SE, Ochiai K, et al. Ras orchestrates exit from the cell cycle and light-chain recombination during early B cell development. *Nat Immunol*. 2009;10(10): 1110-1117.
- Zeng H, Yu M, Tan H, et al. Discrete roles and bifurcation of PTEN signaling and mTORC1-

- mediated anabolic metabolism underlie IL-7-driven B lymphopoiesis. *Sci Adv*. 2018;4(1): eaar5701.
12. Fleming HE, Paige CJ. Pre-B cell receptor signaling mediates selective response to IL-7 at the pro-B to pre-B cell transition via an ERK/MAP kinase-dependent pathway. *Immunity*. 2001;15(4):521-531.
 13. Goetz CA, Harmon IR, O'Neil JJ, Burchill MA, Farrar MA. STAT5 activation underlies il7 receptor-dependent B cell development. *J Immunol*. 2004;172(8):4770-4778.
 14. Jiang Q, Li WQ, Hofmeister RR, et al. Distinct regions of the interleukin-7 receptor regulate different Bcl2 family members. *Mol Cell Biol*. 2004;24(14):6501-6513.
 15. Huntington ND, Labi V, Cumano A, et al. Loss of the pro-apoptotic BH3-only Bcl-2 family member Bim sustains B lymphopoiesis in the absence of IL-7. *Int Immunol*. 2009;21(6): 715-725.
 16. Malin S, McManus S, Cobaleda C, et al. Role of STAT5 in controlling cell survival and immunoglobulin gene recombination during pro-B cell development. *Nat Immunol*. 2010; 11(2):171-179.
 17. Baizan-Edge A, Stubbs BA, Stubbington MJT, et al. IL-7R signaling activates widespread VH and DH gene usage to drive antibody diversity in bone marrow B cells. *Cell Rep*. 2021;36(2):109349.
 18. Mandal M, Powers SE, Maisenschein-Cline M, et al. Epigenetic repression of the Igk locus by STAT5-mediated recruitment of the histone methyltransferase Ezh2. *Nat Immunol*. 2011;12(12):1212-1220.
 19. Puel A, Ziegler SF, Buckley RH, Leonard WJ. Defective IL7R expression in T-B+ NK+ severe combined immunodeficiency. *Nat Genet*. 1998;20(4):394-397.
 20. Giliani S, Mori L, de Saint Basile G, et al. Interleukin-7 receptor alpha (IL-7Ralpha) deficiency: cellular and molecular bases. Analysis of clinical, immunological, and molecular features in 16 novel patients. *Immunity Rev*. 2005;203(1):110-126.
 21. Prieyl JA, LeBien TW. Interleukin 7 independent development of human B cells. *Proc Natl Acad Sci U S A*. 1996;93(19):10348-10353.
 22. Johnson SE, Shah N, Panoskaltis-Mortari A, LeBien TW. Murine and human IL-7 activate STAT5 and induce proliferation of normal human pro-B cells. *J Immunol*. 2005;175(11): 7325-7331.
 23. Malaspina A, Moir S, Ho J, et al. Appearance of immature/transitional B cells in HIV-infected individuals with advanced disease: correlation with increased IL-7. *Proc Natl Acad Sci U S A*. 2006;103(7):2262-2267.
 24. Johnson SE, Shah N, Bajer AA, LeBien TW. IL-7 activates the phosphatidylinositol 3-kinase/AKT pathway in normal human thymocytes but not normal human B cell precursors. *J Immunol*. 2008;180(12):8109-8117.
 25. Parrish YK, Baez I, Milford T-A, et al. IL-7 Dependence in human B lymphopoiesis increases during progression of ontogeny from cord blood to bone marrow. *J Immunol*. 2009;182(7):4255-4266.
 26. Milford T-AM, Su RJ, Francis OL, et al. TSLP or IL-7 provide an IL-7R α signal that is critical for human B lymphopoiesis. *Eur J Immunol*. 2016;46(9):2155-2161.
 27. Rother MB, Jensen K, van der Burg M, et al. Decreased IL7R α and TdT expression underlie the skewed immunoglobulin repertoire of human B-cell precursors from fetal origin. *Sci Rep*. 2016;6:33924.
 28. Shochat C, Tal N, Bandapalli OR, et al. Gain-of-function mutations in interleukin-7 receptor- α (IL7R) in childhood acute lymphoblastic leukemias. *J Exp Med*. 2011; 208(5):901-908.
 29. Yokoyama K, Yokoyama N, Izawa K, et al. In vivo leukemogenic potential of an interleukin 7 receptor α chain mutant in hematopoietic stem and progenitor cells. *Blood*. 2013;122(26):4259-4263.
 30. Almeida ARM, Neto JL, Cachucho A, et al. Interleukin-7 receptor α mutational activation can initiate precursor B-cell acute lymphoblastic leukemia. *Nat Commun*. 2021; 12(1):7268.
 31. Thomas KR, Allenspach EJ, Camp ND, et al. Activated interleukin-7 receptor signaling drives B-cell acute lymphoblastic leukemia in mice. *Leukemia*. 2022;36(1):42-57.
 32. Geron I, Savino AM, Fishman H, et al. An instructive role for interleukin-7 receptor α in the development of human B-cell precursor leukemia. *Nat Commun*. 2022;13(1):659.
 33. Haddad E, Leroy S, Buckley RH. B-cell reconstitution for SCID: should a conditioning regimen be used in SCID treatment? *J Allergy Clin Immunol*. 2013;131(4):994-1000.
 34. Gaspar HB, Qasim W, Davies EG, Rao K, Amrolia PJ, Veys P. How I treat severe combined immunodeficiency. *Blood*. 2013; 122(23):3749-3758.
 35. Wentink MWJ, Kalina T, Perez-Andres M, et al. Delineating human B cell precursor development with genetically identified PID cases as a model. *Front Immunol*. 2019;10:2680.
 36. Kraus H, Kaiser S, Aumann K, et al. A feeder-free differentiation system identifies autonomously proliferating B cell precursors in human bone marrow. *J Immunol*. 2014; 192(3):1044-1054.
 37. Stuart T, Butler A, Hoffman P, et al. Comprehensive integration of single-cell data. *Cell*. 2019;177(7):1888-1902.e21.
 38. Street K, Rizzo D, Fletcher RB, et al. Slingshot: cell lineage and pseudotime inference for single-cell transcriptomics. *BMC Genomics*. 2018;19(1):477.
 39. Van den Berge K, Roux de Bézieux H, Street K, et al. Trajectory-based differential expression analysis for single-cell sequencing data. *Nat Commun*. 2020;11(1):1201.
 40. de Bézieux HR, Van den Berge K, Street K, Dudoit S. Trajectory inference across multiple conditions with condiments: differential topology, progression, differentiation, and expression. *bioRxiv*. Preprint posted online 10 March 2021. <https://doi.org/10.1101/2021.03.09.433671>
 41. Miller SA, Policastro RA, Sriramkumar S, et al. LSD1 and aberrant dna methylation mediate persistence of enteroendocrine progenitors that support BRAF-mutant colorectal cancer. *Cancer Res*. 2021;81(14):3791-3805.
 42. van der Burg M, Kreyenberg H, Willasch A, et al. Standardization of DNA isolation from low cell numbers for chimerism analysis by PCR of short tandem repeats. *Leukemia*. 2011;25(9):1467-1470.
 43. IJspeert H, Wentink M, van Zessen D, et al. Strategies for B-cell receptor repertoire analysis in primary immunodeficiencies: from severe combined immunodeficiency to common variable immunodeficiency. *Front Immunol*. 2015;6:157.
 44. van Schouwenburg PA, IJspeert H, Pico-Knijnenburg I, et al. Identification of COVID patients with defects in immune repertoire formation or specification. *Front Immunol*. 2018;9:2545.
 45. van Dongen JJM, Langerak AW, Brüggemann M, et al. Design and standardization of PCR primers and protocols for detection of clonal immunoglobulin and T-cell receptor gene recombinations in suspect lymphoproliferations: report of the BIOMED-2 Concerted Action BMH4-CT98-3936. *Leukemia*. 2003;17(12):2257-2317.
 46. Warren RL, Freeman JD, Zeng T, et al. Exhaustive T-cell repertoire sequencing of human peripheral blood samples reveals signatures of repertoire selection and a directly measured repertoire size of at least 1 million clonotypes. *Genome Res*. 2011;21(5):790-797.
 47. IJspeert H, van Schouwenburg PA, van Zessen D, Pico-Knijnenburg I, Stubbs AP, van der Burg M. antigen receptor galaxy: a user-friendly, web-based tool for analysis and visualization of T and B cell receptor repertoire data. *J Immunol*. 2017;198(10):4156-4165.
 48. Alamyar E, Duroux P, Lefranc M-P, Giudicelli V. IMGT® tools for the nucleotide analysis of immunoglobulin (IG) and T cell receptor (TR) V-(D)-J repertoires, polymorphisms, and IG mutations: IMGT/V-QUEST and IMGT/HighV-QUEST for NGS. *Methods Mol Biol*. 2012;882:569-604.
 49. Boyd SD, Marshall EL, Merker JD, et al. Measurement and clinical monitoring of human lymphocyte clonality by massively parallel VDJ pyrosequencing. *Sci Transl Med*. 2009;1(12):12ra23.
 50. Ochiai K, Maisenschein-Cline M, Mandal M, et al. A self-reinforcing regulatory network triggered by limiting IL-7 activates pre-BCR signaling and differentiation. *Nat Immunol*. 2012;13(3):300-307.
 51. Itoh-Nakadai A, Hikota R, Muto A, et al. The transcription repressors Bach2 and Bach1 promote B cell development by repressing the myeloid program. *Nat Immunol*. 2014; 15(12):1171-1180.

52. Revilla-I-Domingo R, Bilic I, Vilagos B, et al. The B-cell identity factor Pax5 regulates distinct transcriptional programmes in early and late B lymphopoiesis. *EMBO J*. 2012; 31(14):3130-3146.
53. Li R, Cauchy P, Ramamoorthy S, Boller S, Chavez L, Grosschedl R. Dynamic EBF1 occupancy directs sequential epigenetic and transcriptional events in B-cell programming. *Genes Dev*. 2018;32(2):96-111.
54. Zehentmeier S, Lim VY, Ma Y, et al. Dysregulated stem cell niches and altered lymphocyte recirculation cause B and T cell lymphopenia in WHIM syndrome. *Sci Immunol*. 2022;7(75):eabo3170.
55. Lim VY, Feng X, Miao R, et al. Mature B cells and mesenchymal stem cells control emergency myelopoiesis. *Life Sci Alliance*. 2023;6(4):e202301924.
56. Long EO, Strubin M, Wake CT, et al. Isolation of cDNA clones for the p33 invariant chain associated with HLA-DR antigens. *Proc Natl Acad Sci U S A*. 1983;80(18):5714-5718.
57. Claesson L, Larhammar D, Rask L, Peterson PA. cDNA clone for the human invariant gamma chain of class II histocompatibility antigens and its implications for the protein structure. *Proc Natl Acad Sci U S A*. 1983;80(24):7395-7399.
58. Leng L, Metz CN, Fang Y, et al. MIF signal transduction initiated by binding to CD74. *J Exp Med*. 2003;197(11):1467-1476.
59. Klasen C, Ohl K, Sternkopf M, et al. MIF promotes B cell chemotaxis through the receptors CXCR4 and CD74 and ZAP-70 signaling. *J Immunol*. 2014;192(11):5273-5284.
60. Shachar I, Flavell RA. Requirement for invariant chain in B cell maturation and function. *Science*. 1996;274(5284):106-108.
61. Gore Y, Starlets D, Maharshak N, et al. Macrophage migration inhibitory factor induces B cell survival by activation of a CD74-CD44 receptor complex. *J Biol Chem*. 2008;283(5):2784-2792.
62. Bucala R, Shachar I. The integral role of CD74 in antigen presentation, MIF signal transduction, and B cell survival and homeostasis. *Mini Rev Med Chem*. 2014; 14(14):1132-1138.
63. Fistonich C, Zehentmeier S, Bednarski JJ, et al. Cell circuits between B cell progenitors and IL-7+ mesenchymal progenitor cells control B cell development. *J Exp Med*. 2018; 215(10):2586-2599.
64. Karin M, Liu Z G, Zandi E. AP-1 function and regulation. *Curr Opin Cell Biol*. 1997;9(2): 240-246.
65. Liebermann DA, Gregory B, Hoffman B. AP-1 (Fos/Jun) transcription factors in hematopoietic differentiation and apoptosis. *Int J Oncol*. 1998;12(3):685-700.
66. Ubieta K, Garcia M, Grötsch B, et al. Fra-2 regulates B cell development by enhancing IRF4 and Foxo1 transcription. *J Exp Med*. 2017;214(7):2059-2071.
67. Peralta-Zaragoza O, Recillas-Targa F, Madrid-Marina V. Terminal deoxynucleotidyl transferase is down-regulated by AP-1-like regulatory elements in human lymphoid cells. *Immunology*. 2004;111(2):195-203.
68. Lin H, Grosschedl R. Failure of B-cell differentiation in mice lacking the transcription factor EBF. *Nature*. 1995; 376(6537):263-267.
69. Nutt SL, Heavey B, Rolink AG, Busslinger M. Commitment to the B-lymphoid lineage depends on the transcription factor Pax5. *Nature*. 1999;401(6753):556-562.
70. Nutt SL, Kee BL. The transcriptional regulation of B cell lineage commitment. *Immunity*. 2007;26(6):715-725.
71. Rothenberg EV. Transcriptional control of early T and B cell developmental choices. *Annu Rev Immunol*. 2014;32:283-321.
72. Dias S, Silva H Jr, Cumano A, Vieira P. Interleukin-7 is necessary to maintain the B cell potential in common lymphoid progenitors. *J Exp Med*. 2005;201(6): 971-979.
73. Schwartz V, Lue H, Kraemer S, et al. A functional heteromeric MIF receptor formed by CD74 and CXCR4. *FEBS Lett*. 2009;583(17):2749-2757.
74. Lee RD, Munro SA, Knutson TP, LaRue RS, Heltemes-Harris LM, Farrar MA. Single-cell analysis identifies dynamic gene expression networks that govern B cell development and transformation. *Nat Commun*. 2021;12(1): 6843.
75. Hirokawa S, Sato H, Kato I, Kudo A. EBF-regulating Pax5 transcription is enhanced by STAT5 in the early stage of B cells. *Eur J Immunol*. 2003;33(7):1824-1829.
76. Roessler S, Györy I, Imhof S, et al. Distinct promoters mediate the regulation of Ebf1 gene expression by interleukin-7 and Pax5. *Mol Cell Biol*. 2007;27(2):579-594.
77. Decker T, Pasca di Magliano M, McManus S, et al. Stepwise activation of enhancer and promoter regions of the B cell commitment gene Pax5 in early lymphopoiesis. *Immunity*. 2009;30(4):508-520.
78. Roychoudhuri R, Clever D, Li P, et al. BACH2 regulates CD8+ T cell differentiation by controlling access of AP-1 factors to enhancers. *Nat Immunol*. 2016;17(7): 851-860.
79. Vierbuchen T, Ling E, Cowley CJ, et al. AP-1 transcription factors and the BAF complex mediate signal-dependent enhancer selection. *Mol Cell*. 2017;68(6):1067-1082. e12.
80. Lankester AC, Albert MH, Booth C, et al. EBMT/ESID inborn errors working party guidelines for hematopoietic stem cell transplantation for inborn errors of immunity. *Bone Marrow Transplant*. 2021;56(9): 2052-2062.

© 2023 by The American Society of Hematology. Licensed under Creative Commons Attribution-NonCommercial-NoDerivatives 4.0 International (CC BY-NC-ND 4.0), permitting only noncommercial, nonderivative use with attribution. All other rights reserved.